The Canadian Mineralogist
Vol. 50, pp. 295-312 (2012)
DOI: 10.3749/canmin.50.2.295

CUPROMAKOPAVONITE, $Cu_8Ag_3Pb_4Bi_{19}S_{38}$, A NEW MINERAL SPECIES, ITS CRYSTAL STRUCTURE AND THE CUPROPAVONITE HOMOLOGOUS SERIES

DAN TOPA[§]

Department of Materials Research and Physics, Paris–Lodron University of Salzburg, Hellbrunnerstrasse 34, A–5020, Salzburg, Austria

EMIL MAKOVICKY

Department of Geography and Geology, University of Copenhagen, Østervoldgade 10, DK–1350, Copenhagen K, Denmark

GHEORGHE ILINCA

Department of Mineralogy, University of Bucharest, Bd. N. Bălcescu, 1, RO–010041, Bucharest, Romania

HERBERT DITTRICH

Department of Materials Research and Physics, Paris–Lodron University of Salzburg, Hellbrunnerstrasse 34, A–5020, Salzburg, Austria

ABSTRACT

Cupromakopavonite, ideally $Cu_8Ag_3Pb_4Bi_{19}S_{38}$, is a new mineral species found in quartz veins at the scheelite deposit Felbertal, Salzburg Province, Austria. It is associated with makovickyite, oversubstituted krupkaite (bd_{55}), hodrušite, and kupčikite. The mineral is opaque and grey with a metallic luster; it is brittle without any discernible cleavage. In reflected light, it is greyish white, the bireflectance is weak, and the anisotropy is moderate in air and strong in oil. Internal reflections are absent. The reflectance data (%, air) are: 42.9, 46.6 at 470 nm, 42.1, 46.5 at 546 nm, 41.3, 45.8 at 589 nm and 40.2, 45.1 at 650 nm. The average results of 15 electron-microprobe analyses are: Cu 7.29(6), Ag 5.48(4), Pb 8.84(14), Cd 0.39(6), Bi 59.9(2), S 17.90(6), total 99.80(23) wt.%, corresponding to $Cu_{7.82}Ag_{3.46}Pb_{2.91}Cd_{0.24}Bi_{19.53}S_{38.05}$ (on the basis of *Me* + S = 72 *apfu*). The simplified formula, $Cu_8Ag_3Pb_4Bi_{19}S_{38}$, is in accordance with the results of our crystal-structure analysis. The density, 6.85 g/cm^3, was calculated using the ideal (structural) formula. Cupromakopavonite has a monoclinic cell with *a* 13.380(2), *b* 4.0007(6), *c* 31.083(4) Å, β 93.064(2)°, *V* 1661.5(4) Å^3, space group *C*2/*m*, and *Z* = 1. The strongest eight lines in the (calculated) powder-diffraction pattern [*d* in Å(I)*hkl*] are: 3.607(57)(207), 3.457(99)($\bar{1}$14), 3.436(37)($\bar{2}$08), 3.340(34)($\bar{4}$01), 2.953(28)(311), 2.874(33)($\bar{2}$0$\underline{10}$), 2.834(100)(313) and 2.256(29)(11$\underline{11}$). The crystal structure was refined to $R = 4.53\%$ and $wR = 6.0\%$ for 1834 reflections [$F_o > 4\sigma(F_o)$]. Our crystal-structure determination reveals that the unusually high value of the *c* parameter results from: (1) regular alternation of pavonite-like N = 4 and N = 5 layers in the structure, (2) regularly oriented distribution of the pairs of Bi pyramids and pairs of Pb–Bi prisms in the thin slabs of the structure, and (3) the appearance of a new three-coordinated Cu site instead of the octahedrally coordinated Ag site in the thin slabs. Cupromakopavonite is the N = 4.5 member of the newly defined cupropavonite homologous series, and its name underscores its close structural relationships to its two neighboring members, cupromakovickyite (N = 4) and cupropavonite (N = 5). We define the structural and chemical properties of this series, with the general, ideal formula, $Cu_8Ag_{2N-6}Pb_4Bi_{2N+10}S_{4N+20}$ for Z = 1, where N is the order of the homologue. It includes N = 7 ("cuproplumbian benjaminite") and N = 8 ("cuproplumbian mummeite").

Keywords: cupromakopavonite, sulfosalt, new mineral species, crystal structure, pavonite homologous series, cupropavonite homologous series, Felbertal deposit, Austria.

§ *E-mail address*: dan.topa@sbg.ac.at

Introduction and History

Among sulfosalts, there are very few families that exhibit spectacular intergrowths produced by exsolution from an originally homogeneous high-temperature phase: the bismuthinite–aikinite solid-solution series (Topa *et al.* 2002), stannite–kësterite and other phases related to chalcopyrite (Moh 1975), and the phases of a broadly defined pavonite homologous series. Several natural occurrences of the members of the latter series, defined by Makovicky *et al.* (1977), exhibit lamellar intergrowths of Cu (and Pb)-poor and Cu (and Pb)-rich phases. The first detailed X-ray-diffraction study of such a pavonite-like material with a lamellar structure revealed the presence of two chemically and structurally different phases. Both phases have almost identical *a* and *b* parameters (13.4 and 4 Å, respectively), whereas the **c** axis is doubled for the Cu (and Pb)-rich phase, named cupropavonite for its Cu-rich content (Karup-Møller & Makovicky 1979, Nuffield 1980). Analogous exsolution phenomena were observed for homologue N = 4, makovickyite (Žák *et al.* 1994, Mumme 1990), and for homologue N = 8, mummeite (Karup-Møller & Makovicky 1992). These cases also were interpreted as the result of decomposition of a homogeneous high-temperature phase. Such exsolution-related pairs represent two mineral species, separated by a definite miscibility-gap. Consequently, the Cu (and Pb)-rich varieties (for N = 4 and 8) received a working modifier, "cuproplumbian" (Karup-Møller & Makovicky 1992, Žák *et al.* 1994).

During a systematic study of mineral specimens from Băiţa Bihor, in the Apuseni Mountains of Romania, and from the Felbertal deposits, Mittelsill, Austria, we found lamellar intergrowths of makovickyite and "cuproplumbian" makovickyite, as well as homogeneous grains of "cuproplumbian" makovickyite. This led to the description of the 29.9 Å variety as a new mineral, cupromakovickyite, and the first determination of a crystal structure of the copper-rich component (Topa & Paar 2008, Topa *et al.* 2008). Although no crystal of (relatively) pure cupropavonite has yet been found, and its crystal structure is still unknown, we provide in the present contribution a formal mineralogical description of a new mineral species, cupromakopavonite, a Cu- and Pb-rich phase structurally positioned between the N = 4 and N = 5 homologues, together with a complete determination of its crystal structure. The current level of structural and chemical knowledge on the Cu–Pb-rich phases based on the generalized principle of pavonite allows us to propose a definition of a new homologous series, crystal-chemically distinct from the "classical" pavonite series, and named after its first known member, cupropavonite.

Research Material

Cupromakopavonite has been detected at the scheelite deposit of Felbertal, Hohe Tauern, Austria, in quartz veins of the K8 orebody, whereas orebodies K1, K3 and K5 contain Cu-free makovickyite (N = 4) and pavonite (N = 5) (Topa 2001, Topa *et al.* 2003b, Topa & Paar 2008). The minerals associated with cupromakopavonite are bismuthinite derivatives in the range aikinite (bd_{92})– krupkaite (bd_{56}), Cu-bearing makovickyite, hodrušite, cuprobismutite, kupčikite, traces of wittichenite, native bismuth, chalcopyrite and pyrrhotite in a matrix of quartz. This mineralization formed by the recrystallization of sulfide and sulfosalt material in quartz veins hosted within felsic gneisses and amphibolites. Recrystallization occurred during the retrograde stage of Alpine metamorphism (Topa *et al.* 2002).

Cupromakopavonite was found only as inclusions in a matrix of oversubstituded krupkaite (bd_{56}). It can appear either as homogeneous grains or as a component in lamellar intergrowths with Cu-bearing makovickyite (Fig. 1). The cupromakopavonite – makovickyite grains represent remnants of larger aggregates with well-defined exsolution lamellae of the two minerals, intensely but selectively replaced by krupkaite (Fig. 1). The extractable homogeneous grains of each phase reach a size of 0.1 mm. The marked places in Figure 1 were investigated by back-scattered electron imaging and quantitative chemical analyses, and used for the mechanical extraction of cupromakopavonite crystals for structural studies.

Physical Properties and Optical Data

Cupromakopavonite is opaque with a metallic luster; it has a grey color and a grey streak. The mineral is brittle, the fracture is uneven, and cleavages or parting were not observed. The density and microhardness could not be measured because no suitable free grains were available. The calculated density based on the ideal formula is 6.78 g/cm^3.

In polarized light, cupromakopavonite is greyish white, without internal reflections. Bireflectance is perceptible in air and moderate in oil, and pleochroism is absent. Anisotropy is moderate in air and strong in oil. The rotation tints between crossed polars are dark bluish grey to yellowish brown for the most strongly anisotropic grains. Reflectance data were obtained in air using a Leitz MPV–SP microscope photometer and a WTiC standard. The observed R_{min} and R_{max} values are summarized in Table 1. Both the R_{min} curve and the R_{max} curve are flat, with a weak maximum at 470–500 nm for the R_{max} curve. This maximum is slightly displaced toward longer wavelengths compared to that observed for cupromakovickyite from Felbertal (Topa & Paar 2008).

Chemical Data

Cupromakopavonite and the associated sulfosalt minerals were analyzed using an JEOL Superprobe

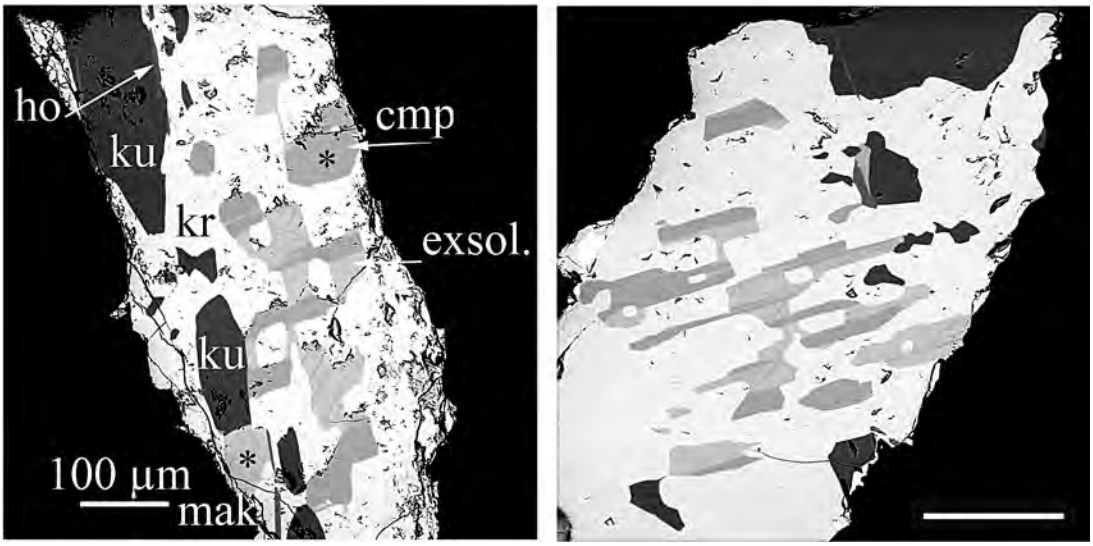

FIG. 1. Back-scattered electron images of exsolution intergrowths of Cu-bearing makovickyite (lighter, *mak*) and cupromakopavonite (darker, *cmp*) heavily replaced by oversubstituted krupkaite, accompanied by subhedral kupčíkite (*ku*) and hodrušite (*ho*). Length of bars is 100 µm in both photographs. The image on the right side makes use of the same conventions as the one with lettering. The grains extracted for the structure studies are marked (*).

JXA–8600 electron microprobe, controlled by PROBE FOR WINDOWS system of programs, and operated at 25 kV and 35 nA, with a beam diameter of 5 µm. Wavelength-dispersion data were collected using the following standards (all synthetic except galena) and emission lines: Bi_2S_3 (Bi*L*α, S*K*α), galena (Pb*L*α), chalcopyrite (Cu*K*α, Fe*K*α), Ag metal (Ag*L*α), CdTe (Cd*L*β, Te*L*α), and Bi_2Se_3 (Se*L*α). The raw data were corrected with the on-line ZAF–4 procedure. The results of the electron-microprobe analyses are compiled in Table 2. The absence of iron, antimony, tellurium, and selenium, and the systematic presence of cadmium (up to 0.5 wt.% in makovickyite, and 0.4 wt.% in cupromakopavonite), have been noted. The empirical formulae of cupromakopavonite and associated makovickyite in Table 2 were calculated on the basis of 18 S *apfu* for makovickyite, in which previous investigations reveal a non-integral and variable number of cations *pfu,* and 72 (*Me* + S) *apfu* for cupromakopavonite, for which a structure investigation (below) suggests an integral number of cations *pfu*. Chemical data for the Cu-bearing makovickyite and cupromakopavonite in Table 2 are plotted in the triangular diagram Bi – Ag – (Pb + Cu) in Figure 2. The chemical composition of associated kupčíkite, hodrušite and cuprobismutite is presented and discussed in detail in Topa *et al*. (2003a, 2003b), whereas bismuthinite derivatives are treated in Topa *et al*. (2002).

TABLE 1. REFLECTANCE DATA (IN AIR) FOR CUPROMAKOPAVONITE FROM FELBERTAL, SALZBURG PROVINCE, AUSTRIA

l (nm)	R_{min} %	R_{max} %	l (nm)	R_{min} %	R_{max} %
400	43.45	45.82	560	42.22	46.06
420	43.28	45.77	580	41.86	45.69
440	43.22	45.29	**589**	**41.34**	**45.78**
460	43.13	46.55	600	41.57	45.71
470	**42.91**	**46.56**	620	41.01	45.25
480	42.86	47.15	640	40.83	44.64
500	42.74	46.94	**650**	**40.24**	**45.13**
520	42.58	46.64	660	40.73	45.28
540	42.39	46.40	680	40.64	44.43
546	**42.1**	**46.46**	700	39.72	44.61

In order to illustrate the associations and the crystal chemistry of the phases involved, we adopted the empirical Bi – Ag – (Pb + Cu) diagram (Karup-Møller & Makovicky 1979), used for pavonite homologues (Fig. 2), to present the combined data for the Felbertal occurrence of cupromakopavonite, makovickyite and pavonite and for those from the Băiţa Bihor occurrence of makovickyite and cupromakovickyite described by Topa & Paar (2008). From the left-hand side of the diagram, the copper-free homologues, makovickyite (N = 4) and pavonite (N = 5) (Topa & Paar 2008) [indicated by empty symbols in Fig. 2] follow the lines of the Ag + Bi ↔ 2Pb substitution (Topa & Paar 2008), parallel to those known from lillianite homologues and from the matildite–galena solid solution. At the end of the N = 4 line, the averaged composition, $Cu_{2.21}Ag_{1.83}$

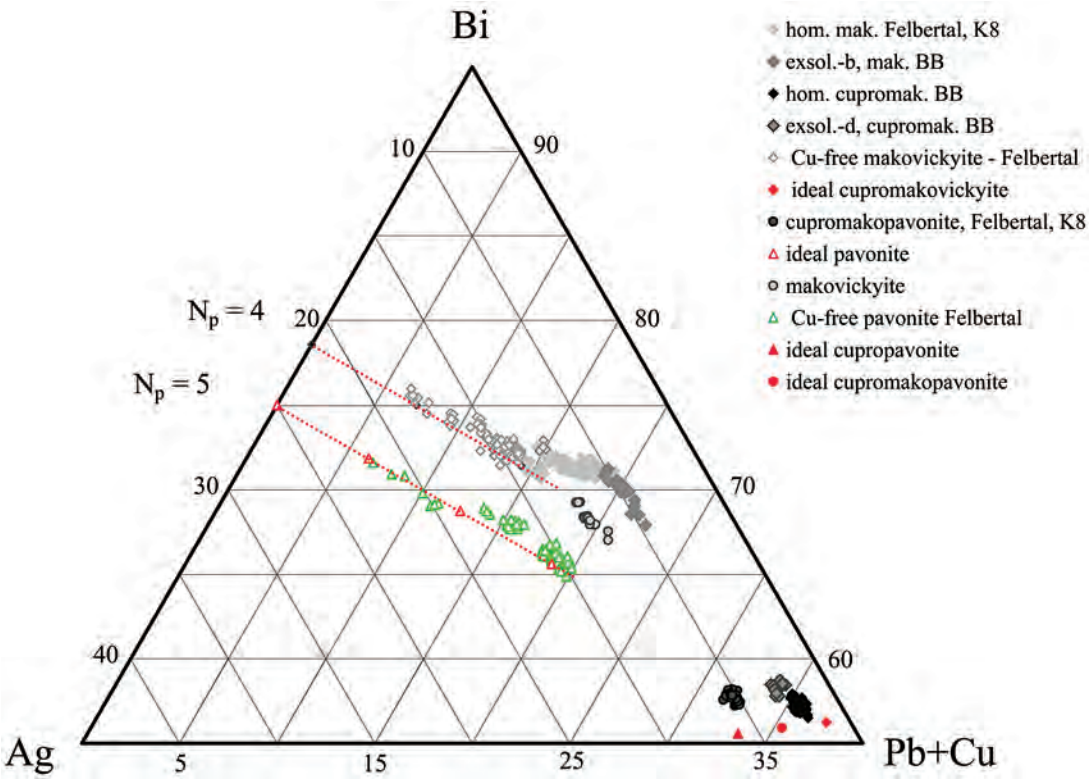

FIG. 2. Positions of selected pavonite homologues, cupromakovickyite and cupromakopavonite in the Ag – Bi – (Pb + Cu) diagram. Red lines indicate the Ag + Bi ↔ 2Pb substitution trends for the N = 4 and 5 pavonite homologues, respectively. Empirical compositions are shown for selected Cu-free makovickyite (N = 4) and pavonite (N = 5) samples, Cu-bearing (homogeneous) makovickyite from Felbertal, and of the makovickyite – cupromakovickyite and makovickyite – cupromakopavonite exsolution pairs from Băiţa Bihor (BB) and Felbertal (K8 and other orebodies, respectively). Abbreviations: *hom*: homogeneous, *mak*: makovickyite, *cupromak*: cupromakovickyite, *exsol*: exsolved lamellae, *b*: bright, *d*: dark.

$Pb_{0.48}Cd_{0.15}Bi_{10.21}S_{18}$, for makovickyite in exsolution pair with cupromakopavonite, suggests that 1.17 Cu *apfu* in makovickyite can be considered *substitutional*, compensating for the lack of silver with respect to the ideal formula $Ag_3Bi_{11}S_{18}$; in addition, 1.04 Cu *apfu* is *interstitial* to the fundamental cation sites of the N = 4 homologue. The large cations amount to 10.85 *apfu,* which practically corresponds to the Bi sites of the ideal formula. The presence of 1.17 atoms Cu *pfu* substituting for Ag distorts the substitution trend in the empirical diagram in the direction of the horizontal Cu ↔ Ag substitution line. The presence of interstitial copper, however, exerts the opposite effect, decreasing the amount of Bi present in favor of more Pb in the formula. The resulting position of the phase in the diagram is indicated by filled circles in Figure 2.

Another trend is followed by the copper-containing homogeneous makovickyite from the K8 deposit of Felbertal (Topa & Paar 2008). In comparison to the phase examined above (and quoted in Table 2), this phase has less Ag, less Pb, more Bi and about the same Cu contents. Correspondingly, less interstitial copper is present, and at about 20 at.% (Pb + Cu) of the cation sum, the above-mentioned simple substitution line is abandoned, and a trend toward progressively lower apparent values of N *and* the Cu ↔ Ag substitution begins (light grey lozenges in Fig. 2). The exsolution pair makovickyite–cupromakovickyite from Băiţa Bihor (Topa *et al*. 2008) continues this latter trend. It displays the makovickyite–cupromakovickyite tie-line with the same general orientation as observed by Karup-Møller & Makovicky (1979) for a pavonite–cupropavonite pair.

X-RAY-DIFFRACTION DATA

For our single-crystal investigation, irregular, blade-like fragments were extracted from the polished specimen (Fig. 1). Intensity data were collected on

a Bruker AXS P3 diffractometer operated at 50 kV and 35 mA, equipped with a CCD area detector using graphite-monochromated Mo*K*α radiation. Experimental data are listed in Table 3. The SMART (Bruker AXS 1998a) system of programs was used for unit-cell determination and data collection, SAINT+ (Bruker AXS 1998b) for the reduction of the intensity data, and XPREP (Bruker AXS 1997) for space-group determination and empirical absorption-correction based on pseudo Ψ-scans. The centrosymmetric space-group *C*2/*m*, proposed by the XPREP program, was chosen. It is consistent with the monoclinic symmetry of the lattice and intensity statistics (mean $|E * E - 1| = 1.019$ [expected values: 0.968 for the centrosymmetric case and 0.736 for the non-centrosymmetric case]). The structure of cupromakopavonite was solved by direct methods (program SHELXS, Sheldrick 1997a), which revealed most of the atom-positions. In subsequent cycles of the refinement (program SHELXL, Sheldrick 1997b), remaining atom-positions were deduced from difference-Fourier syntheses by selecting from among the strongest maxima at appropriate distances. Data on X-ray diffraction and the structure refinement are summarized in Table 3. Positional and displacement parameters refined are given in Table 4, selected interatomic distances, in Table 5, and coordination-polyhedron characteristics calculated with IVTON program (Balić-Žunić & Vicković 1996), in Table 6. Tables listing the observed and calculated structure-factors may be obtained from the Depository of Unpublished Data on the Mineralogical Association of Canada website [document Cupromakopavonite CM50_295]. The site labeling and the crystal structure of cupromakopavonite are illustrated in Figures 3 and 4, respectively.

Cupromakopavonite is monoclinic, space group *C*2/*m*, with *a* 13.380(2), *b* 4.0007(6), *c* 31.083(4) Å, β 93.064(2)°, *V* 1661.5(4) Å^3, and *Z* = 1, for a structural formula $Cu_8Ag_3Pb_4Bi_{19}S_{38}$. Its theoretical powder-diffraction pattern (Table 7) was calculated using PowderCell 2.3 software (Kraus & Nolze 1999) for a Debye–Scherrer configuration. We used Cu*K*α radiation (λ = 1.540598 Å), a fixed slit, no correction for anomalous dispersion, and unit-cell parameters, space group, atom positions, site occupancy and anisotropic displacement factors from the refined structure.

Description of the Structure

In the structure of cupromakopavonite, there are five Bi sites, one Ag site, one Pb site, two Cu sites and ten S sites. The site-occupancy factors for the two Cu sites refine to the scattering power of a Cu atom and were subsequently fixed. The site-occupancy factors of two Bi sites (Bi4, Bi5) are significantly lower (indicating the presence of a lighter element) compared with the site-occupancy factors of the remaining ones (Bi1, Bi2 and Bi3), refined as pure Bi sites.

The structure (Fig. 4) is composed of three types of layer. The A layers, N = 4, are composed of coordination octahedra, four octahedra thick if counted along the $(100)_{PbS}$ plane diagonal to the layers themselves. The B layers are thinner and asymmetric; they accommodate

TABLE 2. AVERAGE RESULTS OF ELECTRON-MICROPROBE ANALYSES OF CUPROMAKOPAVONITE FROM FELBERTAL, AUSTRIA, AND OF OTHER HOMOLOGUES QUOTED

No.	mineral	NA	Cu	Ag	Pb	Cd	Bi	S	total	N_P	N_{P1}	N_{P2}	N_{P3}	Σ*Me*	*ch*	*ev*
1	cupromakopavonite	17	7.29	5.48	8.84	0.39	59.90	17.90	99.80	4.5	3.50	5.45	*4.48*	33.91	0.08	0.08
			0.06	0.04	0.14	0.06	0.20	0.06	0.23							
2	makovickyite	26	4.44	6.23	3.12	0.52	67.24	18.19	99.77	4	3.05	*4.11*	3.58	14.88	-0.08	-0.21
			0.23	0.13	0.50	0.07	0.71	0.06	0.31							
3	cupropavonite	9	6.87	5.90	13.09	0.02	56.71	17.60	100.35	5	4.19	6.18	*5.18*	36.12	0.46	0.44
			0.16	0.09	0.16	0.02	0.30	0.07	0.28							
4	pavonite	8	2.66	9.32	6.23	0.05	64.17	17.65	100.29	5	4.69	*5.45*	5.07	16.80	0.57	0.53
			0.12	0.18	0.23	0.02	0.31	0.08	0.09							
5	cuproplumbian mummeite	3	5.14	12.80	7.80	-	57.35	17.43	100.68	8	8.06	10.14	*9.11*	48.43	0.82	0.80
			0.01	0.10	0.10		0.05	0.03	0.31							
6	mummeite	3	0.91	13.50	10.15	-	58.13	17.08	99.95	8	8.82	*9.20*	9.01	22.63	0.39	0.37
			0.01	0.02	0.06		0.32	0.04	0.37							

1) $Cu_{7.82}Ag_{3.46}(Pb_{2.91}Cd_{0.24})_{\Sigma 3.15}Bi_{19.53}S_{38.05}$
2) $Cu_{2.21}Ag_{1.83}(Pb_{0.48}Cd_{0.15})_{\Sigma 0.63}Bi_{10.21}S_{18}$
3) $Cu_{7.84}Ag_{3.97}Pb_{4.59}Cd_{0.01}Bi_{19.68}Sb_{0.03}Se_{0.02}Te_{0.07}S_{39.80}$
4) $Cu_{1.52}Ag_{3.05}Pb_{1.09}Cd_{0.02}Bi_{11.12}Sb_{0.01}Se_{0.02}Te_{0.07}S_{39.80}$
5) $Cu_{7.66}Ag_{11.23}Pb_{3.56}Bi_{25.98}Te_{0.12}S_{51.45}$
6) $Cu_{0.70}Ag_{6.00}Pb_{2.39}Bi_{13.54}Te_{0.07}S_{25.93}$

The compositions are expressed in wt.%. NA: number of analyses. The standard deviation is shown on the second line. The chemical homologue numbers N_{P1}, N_{P2} and N_{P3} were calculated after Karup-Møller & Makovicky (1979). Empirical formulae were calculated on the basis of *Me* + S = 72 *apfu* for cupromakopavonite, S = 18 *apfu* for makovickyite, *Me* + S = 76 *apfu* for cupropavonite, S = 20 *apfu* for pavonite and *Me* + S = 100 *apfu* for cuproplumbian mummeite, S = 26 *apfu* for mummeite.

Cu, Pb and Bi. The C layers of octahedra, N = 5, are five octahedra thick if counted along the $(100)_{PbS}$ plane, with Ag in the central octahedron (Fig. 4). It differs from all members of the series with known crystal-structures, in which only one value of N is valid for all layers of octahedra, even if the details of their occupancy may differ, *e.g.*, in cupromakovickyite (Topa *et al.* 2008).

In the A layers, both the marginal coordination octahedra Bi4 and the central ones Bi5 are partly replaced by Ag (Table 4). In the broader layers (C), silver is concentrated in the central Ag octahedron, whereas both the marginal Bi2 octahedra and the central Bi1 octahedra (Fig. 4) were refined as pure Bi. The asymmetric distribution of bond lengths and the eccentricity of these two bismuth positions are consistent with their position at the margins of the layer (Tables 5, 6). Characteristics for the Bi4 and Bi5 sites (Tables 5, 6) are closest to those of the marginal Bi2 site.

The B layers separate the A and C layers. They contain columns with a configuration of flat octahedra, in which only one wall of octahedra is occupied by approximately trigonal–planar Cu2 with a very long additional distance to S4 (Table 5, Fig. 4). A tetrahedral space between adjacent octahedra in the [010] column of foreshortened octahedra is occupied by tetrahedrally coordinated Cu1, situated on the same level as S5 and S6 (Fig. 4). Both Cu positions were refined as being fully occupied, unlike those in such columns in Cu-containing pavonite homologues. The octahedra themselves can be considered vacant. These columns of octahedra are interspersed along [100] by [010] columns of an oriented pair of large cations: a column of square-coordination pyramids of Bi joined sideways with a column of capped trigonal coordination prisms of Pb. The former is typical of members of a pavonite homologous series, but the latter is much closer to the bicapped coordination prisms of Pb in lillianite homologues. Polyhedron characteristics of the Pb position (the shortest bond-distances and smallest bond-valence sum, Table 6) suggest that this position contains an admixture of Bi.

The Pb polyhedra from two adjacent B layers face one and the same A layer with N = 4; the Bi polyhedra from adjacent B layers face the next, crystallographically distinct C layer with N = 5. Both Cu1 and Cu2 in the B layer are strictly oriented toward their respective sides of the B layer, in agreement with the Pb–Bi separation and order in this layer. Atom Cu1 is situated on the Bi-populated side of the thin B layer, whereas Cu2 is on the Pb-populated side of this layer. The observed scheme of Cu bonding is found also in cupromakovickyite (Topa *et al.* 2008), $Cu_4Bi_4S_9$ (Takéuchi & Ozawa 1974, Bente & Kupčík 1984) and $Cu_4Bi_4Se_9$ (Makovicky *et al.* 2002). It is an ordered and much simplified version of the statistically disordered distribution of Cu in the columns of octahedra in B-type layers in synthetic pavonite homologues N = 3 and N = 4 (Tomeoka *et al.* 1980) and in makovickyite (Mumme 1990, Žák *et al.* 1994, Topa *et al.* 2008), in which the B layer contains only double columns of Bi coordination pyramids, *i.e.*, both its surfaces have the same Bi-based configuration.

Cupromakopavonite is the first natural phase found to combine a 1:1 ratio of two intergrown layers of a different thickness of a type found in the pavonite homologous series. The other case of such a 1:1 intergrowth is the unpublished mention of a regular intergrowth of the third and fourth member of the pavonite homologous series found among synthetic Pb-substituted copper–bismuth sulfosalts by K. Mariolacos (oral commun.). More complicated intergrowths of diverse

TABLE 3. CUPROMAKOPAVONITE: EXPERIMENTAL DETAILS ABOUT THE STRUCTURE REFINEMENT, AND CRYSTAL DATA

Crystal data	
Chemical formula	$Cu_{7.82}Pb_{2.91}Cd_{0.24}Ag_{3.46}Bi_{19.53}S_{38.05}$
Chemical formula weight	6849.6
Crystal system	Monoclinic
Space group	*C2/m*
Cell parameters	
a, *b*, *c* (Å)	13.3801(19), 4.0007(6), 31.083(4)
β (°)	93.064(2)
V (Å^3)	1661.5(4)
Z	1
D_x (mg m^{-3})	6.85
No. of reflections for cell parameters	3105
μ (mm^{-1})	64.7
Crystal morphology	irregular
Crystal size (mm)	0.02 × 0.04 × 0.08
Crystal color	black
Data collection	
T_{min}, T_{max}	0.108, 0.545
No. of measured reflections	7811
No. of independent reflections	2215
No. of observed reflections	1834 for which $F_o > 4\sigma(F_o)$
Criterion for observed reflections	$I > 2\sigma(I)$
R_{int}, R_{sigma} (%)	9.78, 7.54
θ_{max} (°)	28.29
Range of *h, k, l*	$-17 \le h \le 17$, $-5 \le k \le 5$, $-40 \le l \le 41$
Refinement	
Refinement on F_o^2	
$R_1[F_o > 4\sigma(F_o)]$ (%)	4.53
$wR(F_o^2)$	6.00
S (*GooF*)	1.018
No. of reflections used	2215
No. of parameters refined	115
Weighting scheme $w = 1/[\sigma^2(F_o^2) + (0.0335P)^2 + 0.0P]$, where $P = (F_o^2 + 2F_c^2)/3$	
$(\Delta/\sigma)_{max}$	0.014
$\Delta\rho_{max}$ (e/Å^3)	3.98 [1.07 Å from Bi3]
$\Delta\rho_{min}$ (e/Å^3)	-3.98 [1.24 Å from Bi3]
Extinction coefficient	0.000000(17)
Source of scattering factors of atoms: *International Tables for Crystallography,* (1992, Vol. C, Tables 4.2.6.8 and 6.1.1.4)	
Computer programs	
Structure solution	*SHELXS97* (Sheldrick 1997a)
Structure refinement	*SHELXL97* (Sheldrick 1997b)

TABLE 4. POSITIONAL AND DISPLACEMENT PARAMETERS OF ATOMS IN CUPROMAKOPAVONITE

ATOM	x	z	sof	U_{eq}	U_{11}	U_{22}	U_{33}	U_{13}
Ag	0	0	0.937(12)	0.034(1)	0.030(1)	0.041(2)	0.031(2)	-0.002(1)
Bi	0	0	0.063(12)	0.034(1)	0.030(2)	0.041(2)	0.031(2)	-0.002(1)
Bi1	0.27808(5)	0.05767(2)	1	0.0138(2)	0.0159(4)	0.0118(3)	0.0137(4)	0.0013(3)
Bi2	0.44173(5)	0.88385(2)	1	0.0133(2)	0.0158(4)	0.0117(3)	0.0126(4)	0.0022(3)
Bi3	0.18026(5)	0.78873(2)	1	0.0181(2)	0.0195(4)	0.0210(4)	0.0133(41)	-0.0031(3)
Bi4	0.42586(6)	0.58778(3)	0.803(8)	0.0207(3)	0.0246(5)	0.0204(5)	0.0170(5)	0.0019(3)
Ag4	0.42586(6)	0.58778(3)	0.197(8)	0.0207(3)	0.0246(5)	0.0204(5)	0.0170(5)	0.0019(3)
Bi5	0.14238(6)	0.53161(3)	0.855(9)	0.0202(3)	0.0208(5)	0.0179(5)	0.0218(5)	-0.0003(3)
Ag5	0.14238(6)	0.53161(3)	0.145(9)	0.0202(3)	0.0208(5)	0.0179(5)	0.0218(5)	-0.0003(3)
Pb	0.28681(6)	0.33522(3)	1	0.0299(2)	0.0349(5)	0.0179(4)	0.0376(5)	0.0080(4)
Cu1	0.0566(2)	0.2257(1)	1	0.0295(6)	0.023(1)	0.029(1)	0.035(21)	-0.009(1)
Cu2	0.4885(2)	0.7134(1)	1	0.0294(6)	0.030(1)	0.016(1)	0.041(2)	-0.010(1)
S1	0.3537(3)	0.9712(2)	1	0.016(1)	0.017(2)	0.017(2)	0.015(3)	0.004(2)
S2	0.0742(4)	0.9215(2)	1	0.023(1)	0.019(2)	0.014(2)	0.034(3)	-0.004(2)
S3	0.1977(3)	0.1365(2)	1	0.0122(9)	0.015(2)	0.015(2)	0.007(2)	0.000(2)
S4	0.4906(3)	0.1940(2)	1	0.0142(9)	0.019(2)	0.015(2)	0.010(2)	0.004(2)
S5	0.2194(3)	0.2482(2)	1	0.0137(9)	0.012(2)	0.014(2)	0.015(2)	-0.001(2)
S6	0.0745(3)	0.7170(2)	1	0.0122(9)	0.014(2)	0.011(2)	0.012(2)	-0.001(2)
S7	0.3553(3)	0.6653(2)	1	0.0166(9)	0.017(2)	0.013(2)	0.020(3)	0.002(2)
S8	0.0611(3)	0.6065(2)	1	0.0170(9)	0.018(2)	0.016(2)	0.016(3)	-0.001(2)
S9	0.2245(4)	0.4403(2)	1	0.023(1)	0.019(2)	0.015(2)	0.036(3)	-0.004(2)
S10	0.5	0.5	1	0.020(1)	0.022(3)	0.019(3)	0.020(4)	0.000(3)

All $y = 0$, $U_{12} = 0$ and $U_{23} = 0$ by symmetry.

TABLE 5. SELECTED CATION–ANION BOND DISTANCES (Å) IN CUPROMAKOPAVONITE

Ag-		Bi1-		Bi2-		Bi3-	
S2	2.684(6) × 2	S3	2.728(4)	S4	2.627(4)	S6	2.577(4)
S1	2.906(3) × 4	S1	2.783(3) × 2	S3	2.785(3) × 2	S5	2.699(3) × 2
		S2	2.862(4) × 2	S2	2.879(4) × 2	S4	3.106(3) × 2
Cu1-		S1	2.922(5)	S1	3.017(5)	S3	3.415(3) × 2
S5	2.252(5)						
S4	2.379(3) × 2						
S6	2.567(5)	Bi4-		Bi5-		Pb-	
		S7	2.633(5)	S8	2.622(5)	S7	2.759(3) × 2
Cu2-		S8	2.739(3) × 2	S9	2.788(4) × 2	S5	2.805(5)
S7	2.264(5)	S9	2.936(4) × 2	S10	2.898(1) × 2	S6	3.225(3) × 2
S6	2.307(2) × 2	S10	2.953(1)	S9	3.098(6)	S8	3.321(4) × 2
S4	2.879(5)					S9	3.413(6)

$N_{1,2} = 2,3$ combinations were synthesized among Cd–Bi homologues of pavonite (Choe *et al.* 1997).

Mineral Definition, Name and Type Material

Cupromakopavonite is related to cupromakovickyite and to cupropavonite and can be described as a 1:1 intergrowth of slabs from these two phases. According to the orientation of the Pb–Bi pairs, both of those phases contain two types of layers with the same N value, one enclosed between the Pb polyhedra on both its sides, the other surrounded by Bi polyhedra on both its surfaces. In cupromakopavonite, the Pb polyhedra surround the thinner N = 4 layer, whereas the Bi polyhedra surround the thicker N = 5 layer. Thus, cupromakopavonite is a specific combination of selected slabs from the adjacent phases in the system. Its strict structural regularity makes it an independent compound and mineral. Another interpretation of cupromakopavonite is a 1:1 intergrowth of N = 5 pavonite with N = 4 lillianite. A boundary goes through the coordination prisms of Pb, and the columns of octahedra belong to the pavonite layers. It also is the first case where exsolution produces two homologues with different N values, suggesting that the high-temperature phase perhaps contained a disordered mixture of different thicknesses of slab. Both the mineral and its name were approved by the Commission on new Minerals and Names (IMA 2005–036).

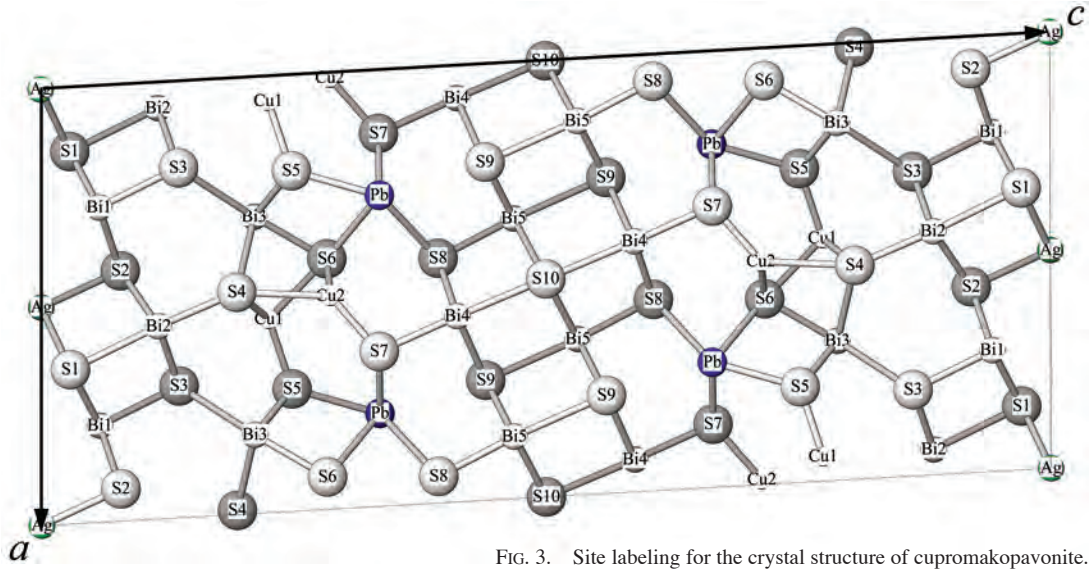

FIG. 3. Site labeling for the crystal structure of cupromakopavonite.

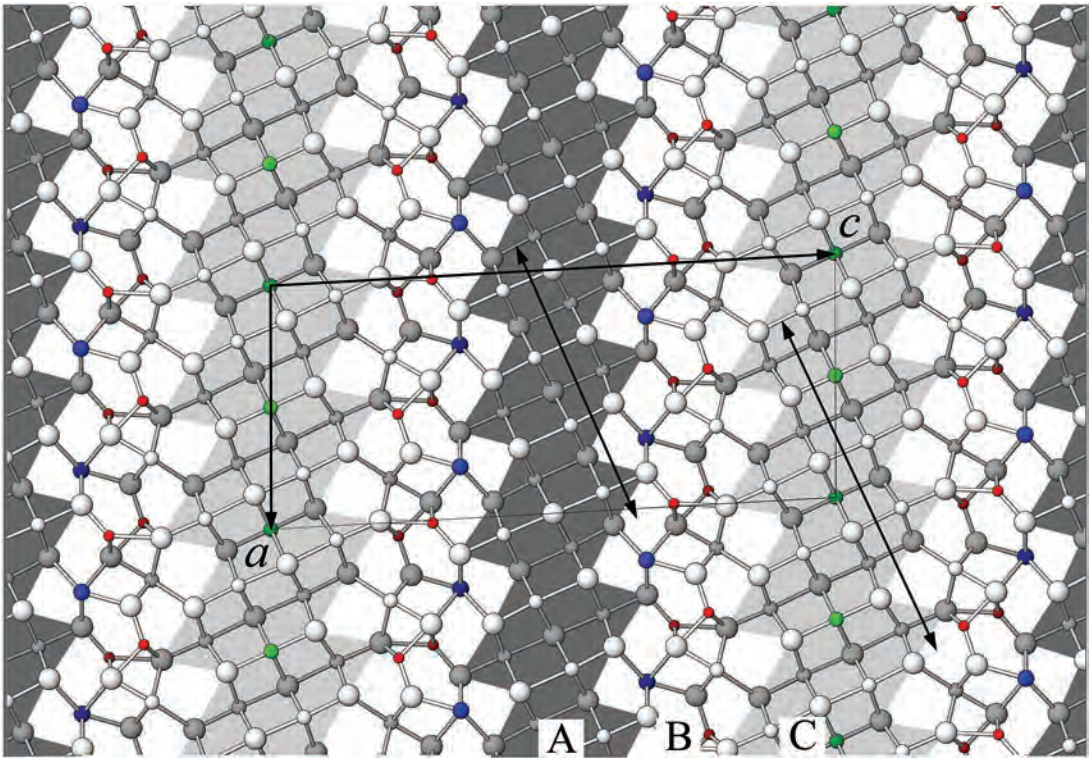

FIG. 4. The crystal structure of cupromakopavonite in projection on (010), with atoms at $y = 0$ (white) and at 0.5 (grey shading), respectively ($b \sim 4$ Å). In the order of decreasing size, circles represent S, Pb (blue), Ag (green), Bi (white) and Cu (red). The two types of thicker layers of octahedra, with N = 4 and N = 5, are shaded in dark and light grey tones, respectively. The A, B and C notation of slabs is explained in the text.

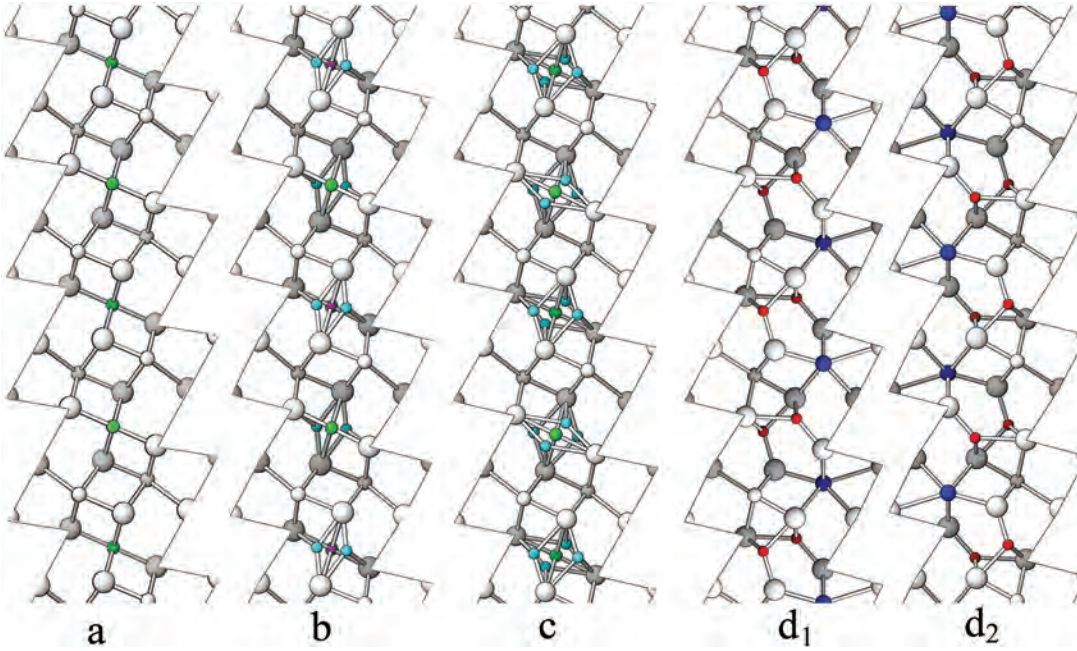

FIG. 5. Selected examples of thinner structural slabs from the crystal structures of pavonite (a, b, and c) and cupropavonite homologues (d_1 and d_2). a) Synthetic pavonite $AgBi_3S_5$ (Makovicky *et al.* 1977); the octahedral Ag site (green) is fully occupied. b) Makovickyite (Topa *et al.* 2008) and c) Cu-bearing benjaminite (D. Topa, unpubl. data); Ag site (green) and Cu sites (blue and red) are partially occupied. d) Two adjacent thin layers d_1 and d_2 in cupromakovickyite and cupromakopavonite (Topa *et al.* 2008, this study); the Pb site (dark blue) and Cu sites (red) with opposite orientations are fully occupied.

Holotype material is deposited under catalog no. 14955 in the reference collection (museum) of the Division of Mineralogy, University of Salzburg, Austria.

THE CUPROPAVONITE HOMOLOGOUS SERIES

In 1977, Makovicky *et al.* defined the pavonite homologous series, with pavonite, ideally $AgBi_3S_5$, benjaminite, ideally $Ag_3Bi_7S_{12}$, two synthetic Cu–Bi sulfosalts, and $PbBi_4S_7$ as homologues with N between 2 and 7. All these phases, with space-group symmetry *C*2/*m,* have a structure composed of two kinds of regularly alternating (001) layers. The layers composed of arrays of slightly distorted coordination octahedra of Bi, Ag and Pb are the (311) slabs of PbS structural archetype of different thickness, which defines the order N of the homologue. The other set of (001) layers has constant topology, composed of [010] columns of coordination octahedra interspersed with double columns of coordination pyramids of bismuth. The columns of octahedra are occupied by octahedrally coordinated Ag (Pb in $PbBi_4S_7$) or variously coordinated partially occupied copper sites. Since then, the pavonite homologous series has undergone considerable expansion in number of homologues and number of elemental combinations that adopt this structure type (Makovicky 1981, 1989, 1997, 2006, Makovicky & Mumme 1979, Mumme & Watts1980, Herbert & Mumme 1981, Mumme 1990, Ilinca & Makovicky 1999, Ferraris *et al.* 2004, Chaplygin *et al.* 2005, Balić-Žunić & Makovicky 2007, Makovicky *et al.* 2010). Although there were several tabulations of the pavonite homologues in these contributions, a comprehensive graphic review of the thicker and thinner layers in these structures, with their individual configurations, has been missing. Figure 5 illustrates important types of thinner layers, with details of their occupancy by Cu and Ag, and Figure 6 shows the configuration of thicker layers for homologues 1 to 8.

Within two years after its definition, a complication of the scheme was found (Karup-Møller & Makovicky 1979) when copper-rich samples of pavonite (N = 5 member of the series) from the Alaska mine, Colorado, were found to display intimate exsolution-induced lamellae having a unit cell with the same space-group but with the *c* parameter of the monoclinic cell doubled compared to that of the associated pavonite: 33.1 Å instead of ~16.4 Å. It was named cupropavonite. In spite of its exsolved nature, Weissenberg data on an exsolved single-crystal aggregate showed good structural order of both components. Similar exsolution-induced

TABLE 6. POLYHEDRON CHARACTERISTICS IN THE CRYSTAL STRUCTURE OF CUPROMAKOPAVONITE

1	2	3	4	5	6	7	8	9
Ag	6	2.832	0.0035	0.0000	0.8784	95.173	30.189	0.991
Bi1	6	2.821	0.0020	0.1127	0.9954	94.083	29.887	2.910
Bi2	6	2.821	0.0025	0.2009	0.9977	94.074	29.870	2.977
Bi3	7	3.045	0.1608	0.4824	0.9739	118.278	37.562	2.905
Bi4	6	2.822	0.0021	0.2126	0.9781	94.100	29.891	3.040
Bi5	6	2.853	0.0063	0.2392	0.9952	97.279	30.771	2.883
Pb	8	3.102	0.0356	0.3488	0.8918	125.010	52.260	2.307
Cu1	4	2.376	0.0382	0.2261	1.0000	56.181	6.620	0.986
Cu2	4	2.447	0.1567	0.5014	0.9996	61.347	6.338	0.997

The polyhedron characteristics used were defined in Balić-Žunić & Makovicky (1996) and Makovicky & Balić-Žunić (1998): 1) atom label, 2) coordination number, 3) radius r_s of a circumscribed sphere, least-squares-fitted to the coordination polyhedron, 4) "volume-based" distortion υ = [V(ideal polyhedron) – V(real polyhedron)] / V(ideal polyhedron). The ideal polyhedron has the same number of ligands. 5) "Volume-based" eccentricity $ECC_V = 1 - [(r_s - \Delta)/r_s]^3$; Δ is the distance between the center of the sphere and the central atom in the polyhedron, 6) "volume-based" sphericity $SPH_V = 1 - 3\sigma_r r_s$; σ_r is a standard deviation of the radius r_s. 7) Volume of the circumscribed sphere, 8) volume of coordination polyhedron, 9) bond-valence sum.

TABLE 7. CALCULATED X-RAY POWDER-DIFFRACTION DATA FOR CUPROMAKOPAVONITE

h	*k*	*l*	*d* Å	I rel.	*h*	*k*	*l*	*d* Å	I rel.
0	0	2	15.52	7	$\bar{3}$	1	10	2.1876	5
2	0	3	5.48	14	$\bar{5}$	1	5	2.1223	17
0	0	6	5.17	3	6	0	4	2.1107	10
$\bar{2}$	0	5	4.67	3	0	0	15	2.0692	6
0	0	7	4.43	4	$\bar{1}$	1	13	2.0406	7
2	0	5	4.43	5	$\bar{6}$	0	7	2.0341	3
$\bar{2}$	0	6	4.20	8	$\bar{5}$	1	7	2.0229	19
1	1	0	3.833	3	1	1	13	2.0127	11
2	**0**	**7**	**3.607**	**57**	5	1	6	2.0096	6
1	1	3	3.576	3	$\bar{2}$	0	15	2.0071	2
$\bar{1}$	**1**	**4**	**3.457**	**99**	6	0	6	2.0068	12
0	0	9	3.449	8	0	2	0	2.0004	28
$\bar{2}$	**0**	**8**	**3.436**	**37**	$\bar{3}$	1	12	1.9878	8
$\bar{4}$	**0**	**1**	**3.340**	**34**	5	1	7	1.9522	3
4	0	1	3.302	3	3	1	12	1.9187	4
1	1	5	3.239	8	$\bar{5}$	1	9	1.9069	6
$\bar{4}$	0	3	3.230	12	5	1	8	1.8923	10
$\bar{1}$	1	6	3.102	6	0	0	17	1.8258	2
3	1	0	2.9762	5	1	1	15	1.8092	3
$\bar{3}$	1	1	2.9727	5	$\bar{3}$	1	14	1.8092	6
3	**1**	**1**	**2.9526**	**28**	4	0	14	1.8033	5
$\bar{3}$	1	2	2.9425	4	$\bar{6}$	0	11	1.7953	4
1	1	7	2.8778	11	5	1	10	1.7700	4
$\bar{2}$	**0**	**10**	**2.8742**	**33**	2	2	7	1.7493	13
3	**1**	**3**	**2.8335**	**100**	3	1	14	1.7483	6
0	0	11	2.8217	4	$\bar{2}$	2	8	1.7287	9
$\bar{3}$	1	4	2.8126	9	7	1	0	1.7227	4
$\bar{3}$	1	6	2.6205	6	$\bar{4}$	2	1	1.7161	9
$\bar{4}$	0	8	2.6010	5	7	1	2	1.7032	6
$\bar{4}$	0	10	2.3369	2	$\bar{4}$	2	3	1.7006	4
$\bar{1}$	1	11	2.2891	7	$\bar{8}$	0	4	1.6510	7
1	**1**	**11**	**2.2558**	**29**	$\bar{2}$	2	10	1.6419	10
4	0	10	2.2155	4	4	0	16	1.6399	2
$\bar{5}$	1	3	2.1927	8	$\bar{4}$	2	8	1.5857	2

aggregates were later found for mummeite, the N = 8 member of the series (Karup-Møller & Makovicky 1992), although doubling of the slightly larger unit-cell of the exsolved component could not be detected. Afterward, Žák *et al.* (1994) found corresponding evidence of lamellar exsolution in Cu-rich varieties of makovickyite, the N = 4 member of the pavonite homologous series. No superstructure could be determined in this case. Finally, Makovicky *et al.* (2010) described the lamellar exsolution-induced textures in Cu-rich benjaminite as well. Further, chemically less well-defined cases of lamellar exsolution were quoted by Karup-Møller & Makovicky (1979).

The structural explanation for the doubled unit cell of the exsolved "cuproplumbian"component had to wait for a suitable material in which the "cuproplumbian" phase was preponderant. [The history of the unusual term "cuproplumbian" and the involvement of the IMA Commission in it is described in Karup-Møller & Makovicky (1979)]. This was supplied by material from the skarn deposit at Băiţa Bihor and from the scheelite deposit at Felbertal, the same deposit that yielded cupromakopavonite. From these deposits, Topa & Paar (2008) defined cupromakovickyite $Cu_8Pb_4Ag_2Bi_{18}S_{36}$, and Topa *et al.* (2008) described its crystal structure. The structural investigation revealed several unusual features. There were two types of N = 4 layers of octahedra present, with partial substitutions by Ag in most Bi octahedra. Lead is concentrated into a Pb polyhedron that, together with the adjacent Bi coordination pyramid, replaces the double column of Bi coordination pyramids seen in pavonite homologues (the latter phases concentrated lead as a substitutional element on the layers of octahedra). Copper does not follow the usual pattern of symmetrically disposed partially occupied tetrahedral and triangular positions, but is concentrated into only two asymmetrically situated sites, entirely analogous to those described here for cupromakopavonite. All these features contribute

to the doubled periodicity along the [001] direction. They were all found in cupromakopavonite, with the exception of a more differentiated Ag–Bi distribution in the N = 5 slab. Comparison of the thin slab configurations of selected examples from among the pavonite homologues with the configuration in cupropavonite homologues is provided in Figure 5. For the thicker slabs, the configurations depicted in Figure 6 apply.

The constancy of these features, present in cupromakovickyite and cupromakopavonite (N = 4 and N = 4.5, respectively), and their pronounced difference from the crystal-chemical features of those substituted pavonite homologues without doubled unit-cells, suggest to us that the "cuproplumbian" varieties form a homologous series of their own. In order to verify this assumption, we undertook, as a working approach, the crystal-structure determination of cupropavonite in a pavonite–cupropavonite intergrowth from the Alaska mine, Colorado, U.S.A. The resulting R value is 0.13. Although it yields an overlap of the two structures, it reveals a clear cupropavonite-like topology with the two Cu sites as described above, located in the region of the column of octahera which, in addition, is populated by octahedrally coordinated Ag. We ascribe the Ag sites to the pavonite component of the mixture because it is geometrically incompatible with the above-mentioned Cu sites. Furthermore, the distribution Pb *versus* Bi and its correlation with Cu distribution are exactly the same as in the above-mentioned pure "cuproplumbian" phases. The Pb site of cupropavonite overlaps partly with the Bi site from the pavonite component, resulting in a "site" with an elongate displacement ellipsoid and somewhat modified *Me*–S distances. The calculated positional parameters for the model of cupropavonite are given in Table 8. The site labeling for proposed cupropavonite structure and its crystal structure are presented in Figure 7 and Figure 8, respectively.

Powder-diffraction data were calculated from a "purified" model of the cupropavonite structure obtained by doubling the *c* unit-cell parameter of a pavonite crystal structure from Felbertal and by arranging the thinner layers to match the ones in cupromakovickyite (Topa & Paar 2008, Topa *et al.* 2008) and in the partially determined cupropavonite structure mentioned above. The unit-cell parameters used for calculation were determined from the graphical construction as *a*

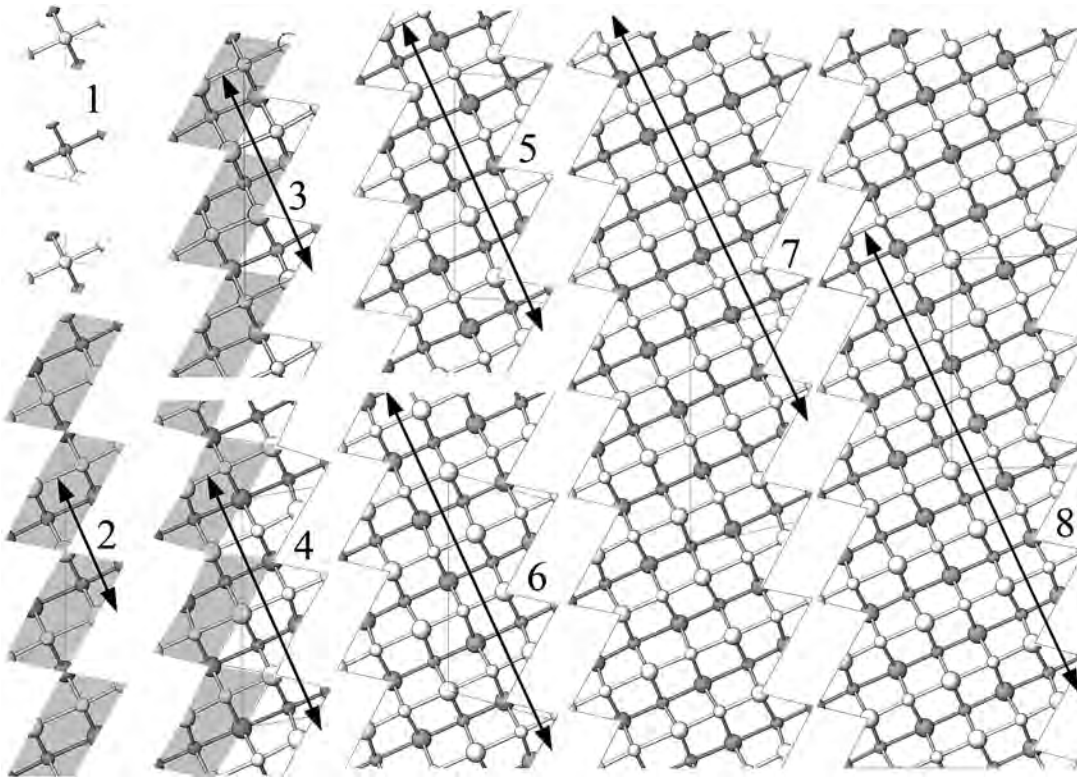

FIG. 6. Configuration of thicker layers of octahedra in the pavonite homologues. Large circles: S, smaller circles: cations. The order of the homologue N_p is determined by the number of octahedra along a diagonal of the layer. The known examples from the cupropavonite homologous series follow the same pattern.

13.254, *b* 4.038, *c* 32.050 Å, β 93.716°. Comparison of calculated data for cupropavonite with the measured powder pattern of cupropavonite from the Alaska mine, Colorado (Karup-Møller & Makovicky 1979) (Table 9) reveals a good agreement, especially for larger and more relevant *d* values. Most of the strongest matching reflections are generated by the thicker layers of octahedra in both the measured and the calculated structures, namely by a set of *I*-centered subcells (*e.g.*, Bi4–Bi5–Ag2–Bi4–Bi5 in Fig. 7) and subordinately, by a set of *C*-centered monoclinic subcells (*e.g.*, S10–Bi5–S8–S8–Bi5–S10–S10 in Fig. 7) (Ilinca & Makovicky 1999). A third set of columns in Table 9 shows the calculated powder-pattern of a "cupropavonite" structure with the unit-cell parameters as above, but from which all thinner layers were eliminated. Only a small number of reflections from the "integral" calculated powder pattern are lost, as a result. Similar *I*- and *C*-centered subcells are present in all pavonite homologues and, therefore, such comparisons of powder data might be less relevant unless indexed patterns and large *00l* reflections with the lowest *l* values are taken into account.

TABLE 8. CALCULATED POSITIONAL PARAMETERS FOR CUPROPAVONITE

ATOM	*x*	*y*	*z*
Ag1	0.000	0.0	0.000
Ag2	0.000	0.0	0.500
Bi1	0.234	0.5	0.056
Bi2	0.468	0.0	0.104
Bi3	0.216	0.0	0.185
Bi4	0.033	0.5	0.391
Bi5	0.265	0.0	0.444
Pb	0.284	0.5	0.305
Cu1	0.070	0.5	0.770
Cu2	0.002	0.0	0.720
S1	0.364	0.0	0.028
S2	0.098	0.0	0.076
S3	0.336	0.5	0.128
S4	0.075	0.5	0.182
S5	0.351	0.5	0.233
S6	0.149	0.0	0.267
S7	0.425	0.0	0.318
S8	0.164	0.0	0.370
S9	0.402	0.5	0.429
S10	0.136	0.5	0.472

Textural evidence of the constancy of structural and crystal-chemical principles in the entire series (Table 10) from N = 4 to N = 8 indicates the same mechanism of exsolution observed for all these values of N (Fig. 9). The two systems of straight exsolution-induced lamellae occur as patches that are mutually exclusive, except for some intersections on their boundaries. From single-crystal diffraction data, Karup-Møller & Makovicky (1979) deduced that the coherent composition-planes of these intergrowths are the (*hkl*) planes with close-packed sulfur atoms in the thicker slabs. For pavonite–cupropavonite, this means planes close to (*1.±1.3*) of pavonite, *i.e.*, (*1.±1.6*) of cupropavonite. Because of small differences in the metrics of the two phases, there is a misalignment of the two lattices on the composition plane, resulting in a small displacement of one component after each lamella of the other component. It is these displacements that make the two, (*113*) and (*1.$\bar{1}$.3*) systems of exsolution lamellae mutually exclusive. These findings apparently hold

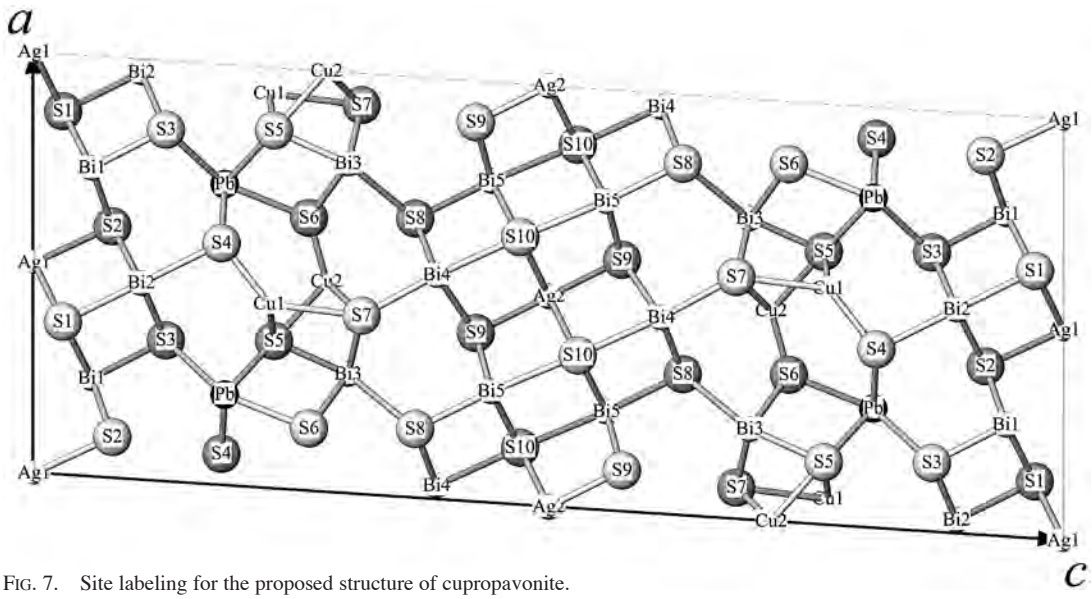

FIG. 7. Site labeling for the proposed structure of cupropavonite.

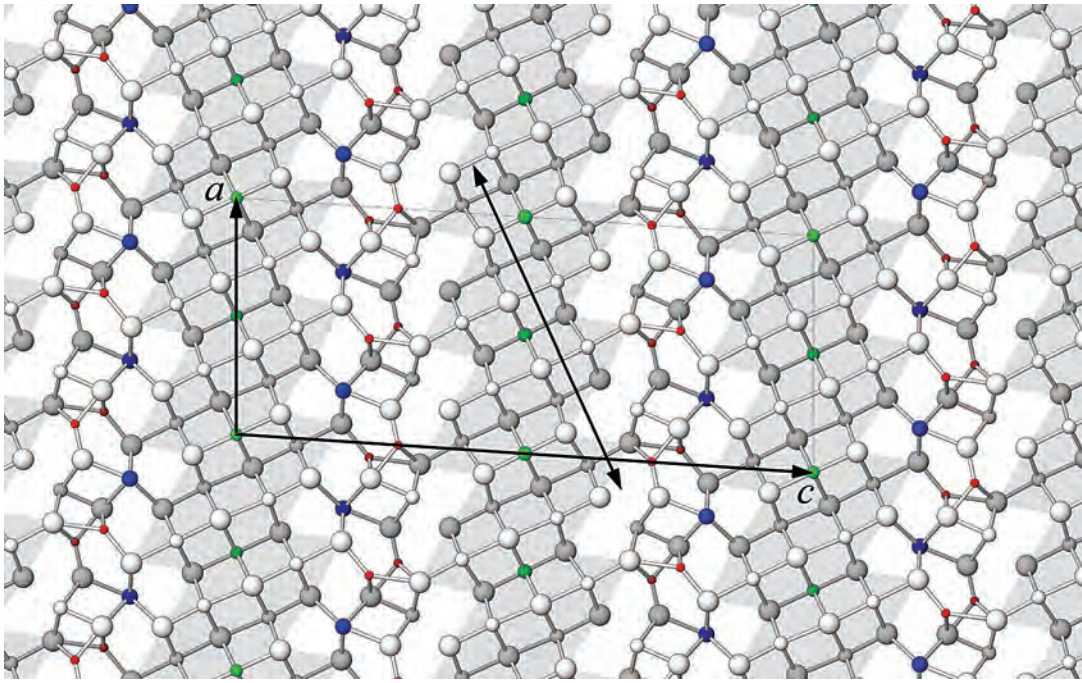

FIG. 8. The hypothetical structure of cupropavonite projected along *b* (~ 4 Å). In order of increasing size, circles represent Cu (red), Bi (white), Ag (green), Pb (blue) and S (white) positions. Void and shaded circles represent atoms at two *y* levels, 2 Å apart. Two types of ^{5}P thicker layers (grey shading) are separated by asymmetric thin cupromakovickyite-like layers (unshaded).

TABLE 9. COMPARISON BETWEEN (1) THE MEASURED X-RAY POWDER PATTERN OF CUPROPAVONITE FROM THE ALASKA MINE* AND (2) THE CALCULATED POWDER PATTERN FOR CUPROPAVONITE DERIVED GRAPHICALLY FROM A PAVONITE CELL DOUBLED ALONG [001] AND WITH THINNER LAYER CONFIGURATION, AS IN CUPROMAKOVICKYITE. SET (3) SHOWS THE SAME SIMULATION BUT WITH ALL ATOMS IN THE THINNER LAYER OMITTED

1					2					3				
h	*k*	*l*	*d* (Å)	I_{calc}	*h*	*k*	*l*	*d* (Å)	I rel.	*h*	*k*	*l*	*d* (Å)	I rel.
0	**0**	**2**	**16.499**	**w**	**0**	**0**	**2**	**16.2158**	**7.14**	**0**	**0**	**2**	**16.2158**	**100**
										0	0	4	8.1079	2.89
2	**0**	**0**	**6.71**		**2**	**0**	**0**	**6.6129**	**4.7**					
2	0	$\bar{1}$	6.655											
					$\bar{2}$	0	2	6.2700	1.94					
					$\bar{2}$	0	3	5.8113	1.88					
					0	0	6	5.4053	4.61	0	0	6	5.4053	3.49
2	**0**	$\bar{4}$	**5.368**	**m/s**	$\bar{2}$	**0**	**4**	**5.2954**	**14.18**	$\bar{2}$	**0**	**4**	**5.2954**	**1.27**
										2	0	4	4.9693	1.78
2	**0**	$\bar{6}$	**4.387**	**m**						$\bar{2}$	**0**	**6**	**4.3247**	**1.03**
					2	0	6	4.0582	14.2					
0	**0**	**8**	**(4.125)**	**w**	**0**	**0**	**8**	**4.0539**	**8.4**					
1	**1**	**0**	**3.854**		**1**	**1**	**0**	**3.8621**	**4.42**	**1**	**1**	**0**	**3.8621**	**1.74**
					1	1	2	3.7411	1.78					
2	**0**	$\bar{8}$	**(3.614)**	**s**	$\bar{2}$	**0**	**8**	**3.5606**	**53.42**	$\bar{2}$	**0**	**8**	**3.5606**	**4.53**
					$\bar{1}$	1	4	3.5126	3.78					
1	**1**	**4**	**3.468**		**1**	**1**	**4**	**3.4614**	**89.82**	**1**	**1**	**4**	**3.4614**	**7.56**

3	1	8	3.376	m									
					2	0	8	3.3605	27.54	2	0	8	3.3605	3.09
					4	0	0	3.3065	26.02	4	0	0	3.3065	2.87
					$\overline{4}$	0	2	3.2817	2.41					
4	0	$\overline{3}$	3.265	m										
					0	0	10	3.2432	4.76					
4	**0**	**$\overline{2}$**	**3.249**	**s**	**4**	**0**	**2**	**3.1995**	**14.05**	**4**	**0**	**2**	**3.1995**	**3.13**
1	**1**	**$\overline{6}$**	**3.182**		**$\overline{1}$**	**1**	**6**	**3.1709**	**5.13**					
1	**1**	**6**	**3.130**	**s**	**1**	**1**	**6**	**3.1146**	**6.67**	**1**	**1**	**6**	**3.1146**	**5**
					$\overline{1}$	1	7	2.9946	2.21					
4	0	$\overline{5}$	3.067	w										
										$\overline{2}$	0	10	2.9894	1.82
3	**1**	**0**	**2.991**	**m**	**3**	**1**	**0**	**2.9778**	**8.63**					
3	1	1	2.968	m										
3	**1**	**$\overline{2}$**	**2.965**	**s**	**$\overline{3}$**	**1**	**2**	**2.9518**	**22.49**	**$\overline{3}$**	**1**	**2**	**2.9518**	**5.84**
					1	1	7	2.9393	1.21					
										3	1	2	2.9063	1.53
4	**0**	**$\overline{6}$**	**2.945**	**m**	**$\overline{4}$**	**0**	**6**	**2.9057**	**1.27**					
2	**0**	**10**	**2.892**	**vs**	**2**	**0**	**10**	**2.8400**	**29.36**	**2**	**0**	**10**	**2.8400**	**6.39**
3	1	3	(2.857)	w/m										
1	1	$\overline{8}$	2.841	m										
					$\overline{3}$	1	4	2.8357	100	$\overline{3}$	1	4	2.8357	12.97
					$\overline{1}$	1	8	2.8231	5.96					
3	1	$\overline{5}$	2.767	m										
					3	1	4	2.7564	8.26					
0	**0**	**12**	**2.750**	**s/m**	**0**	**0**	**12**	**2.7026**	**1.47**					
3	**1**	**5**	**2.684**	**m/w**	**3**	**1**	**5**	**2.6624**	**1.05**					
4	0	$\overline{8}$	2.684	w										
1	1	$\overline{9}$	2.680	w										
										$\overline{3}$	1	6	2.6578	2.29
3	**1**	**6**	**2.584**	**s/m**	**3**	**1**	**6**	**2.5612**	**1.51**					
3	1	$\overline{7}$	(2.574)	w										
					$\overline{2}$	0	12	2.5606	1.93					
					$\overline{1}$	1	10	2.5071	1.81					
					4	0	8	2.4846	6.7					
					2	0	12	2.4469	1.54	2	0	12	2.4469	1.21
					$\overline{4}$	0	10	2.3942	1.77					
					0	0	14	2.3166	1.78					
1	**1**	**$\overline{12}$**	**2.257**	**ws**	**$\overline{1}$**	**1**	**12**	**2.2343**	**23.86**	**$\overline{1}$**	**1**	**12**	**2.2343**	**2.62**
					$\overline{2}$	0	14	2.2319	2.26					
0	0	15	(2.200)	m/w										
					1	1	12	2.1949	10.83					
5	**1**	**2**	**2.198**	**s**	**5**	**1**	**2**	**2.1766**	**13.39**					
					$\overline{6}$	0	4	2.1629	1.89					
4	**0**	**$\overline{12}$**	**2.193**	**ws**	**$\overline{4}$**	**0**	**12**	**2.1623**	**3.73**					
6	0	$\overline{4}$	2.193	m/s										
2	0	14	2.183	m										
5	1	-5	(2.148)	vw										
					3	1	10	2.1471	9.03					
					5	1	4	2.1058	14.17	5	1	4	2.1058	1.22
6	**0**	**$\overline{6}$**	**2.118**	**vs**	**$\overline{6}$**	**0**	**6**	**2.0900**	**9.22**	**$\overline{6}$**	**0**	**6**	**2.0900**	**1.37**
6	**0**	**5**	**2.080**	**w/m**	**1**	**1**	**13**	**2.0777**	**2.09**					
					$\overline{3}$	1	12	2.0463	3.42					
0	**0**	**16**	**2.062**	**s**	**0**	**0**	**16**	**2.0270**	**3.84**					
12	0	15	(2.054)	w										
					0	2	0	2.0191	29.22	0	2	0	2.0191	2.48
					5	1	6	2.0099	22.05	5	1	6	2.0099	4.76
					$\overline{1}$	1	14	2.0034	11.78	$\overline{1}$	1	14	2.0034	4.47
					6	0	6	1.9964	4.52					
6	**0**	**$\overline{8}$**	**2.019**	**vs**	**$\overline{6}$**	**0**	**8**	**1.9915**	**12.74**	**$\overline{6}$**	**0**	**8**	**1.9915**	**2.22**

* Karup-Møller & Makovicky (1979). Thecell parameters for all sets are given in the text.

for all homologues (Fig. 9); only the (*hkl*) values for close-packed planes of sulfur in the structure will differ.

The diffraction evidence of a doubled unit-cell with a strongly expressed subcell, which corresponds to the unit cell of pavonite homologues, is well documented for N = 4, N = 4.5, and partially for N = 5. Lamellar exsolution-induced aggregates in copper-containing benjaminite have not yet been subjected to detailed

X-ray-diffraction studies. Single-crystal diffraction data for the mummeite – "cuproplumbian mummeite" pair ("cupromummeite" is not a recognized mineral species) did not yield evidence of a doubled unit-cell and show continuous [001]* streaks underlying the pavonite-like reciprocal lattice rows parallel to [001]*. The regular alternation of two types of thicker (001) structural layers, known for N = 4 and for N = 5, thus may have broken down, or a consistent orientation of rows of Pb and Bi polyhedra on the surfaces of the thin layers may have been lost. The reciprocal lattice of a still higher homologue than mummeite, observed by Karup-Møller & Makovicky (1992), shows indications of still thicker slabs of octahedra, but its periodicity dissolves in disorder streaks. Whether the lack of a superperiod for N = 8 results from the loss of periodicity due to exces-

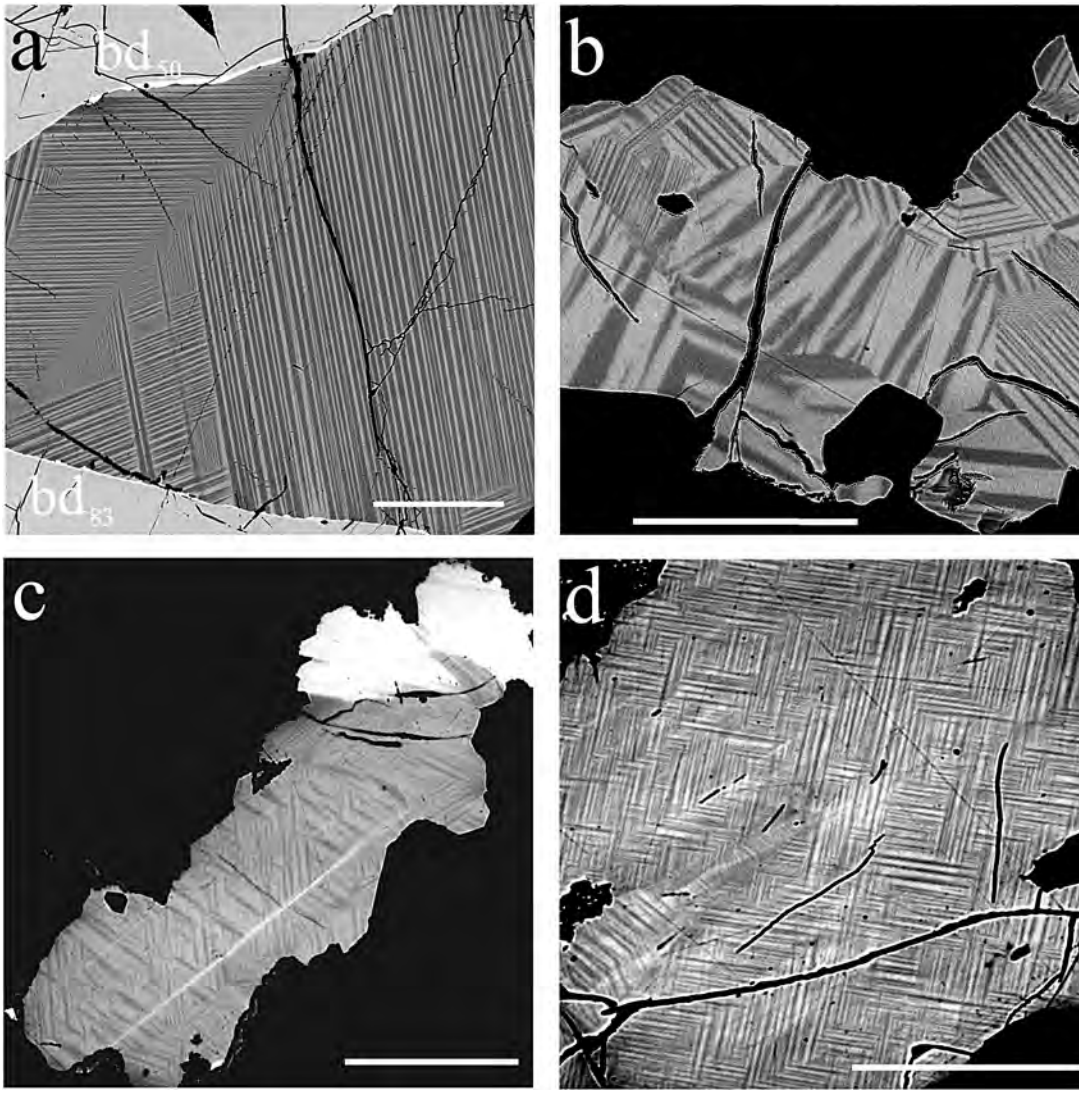

FIG. 9. BSE photographs of exsolution aggregates involving members of the pavonite and cupropavonite homologous series. (a) Makovickyite – cupromakovickyite aggregate from Băiţa Bihor, Romania; (b) pavonite – cupropavonite aggregate from the Alaska mine, Colorado, U.S.A.; (c) benjaminite – cuproplumbian benjaminite aggregate from Erzwies, Austria (Makovicky *et al.* 2010); (d) mummeite – cuproplumbian mummeite aggregate from the Alaska mine, Colorado. In each image, the differences in the thickness of exsolution lamellae are primarily caused by their orientation. The length of the bars is 100 μm.

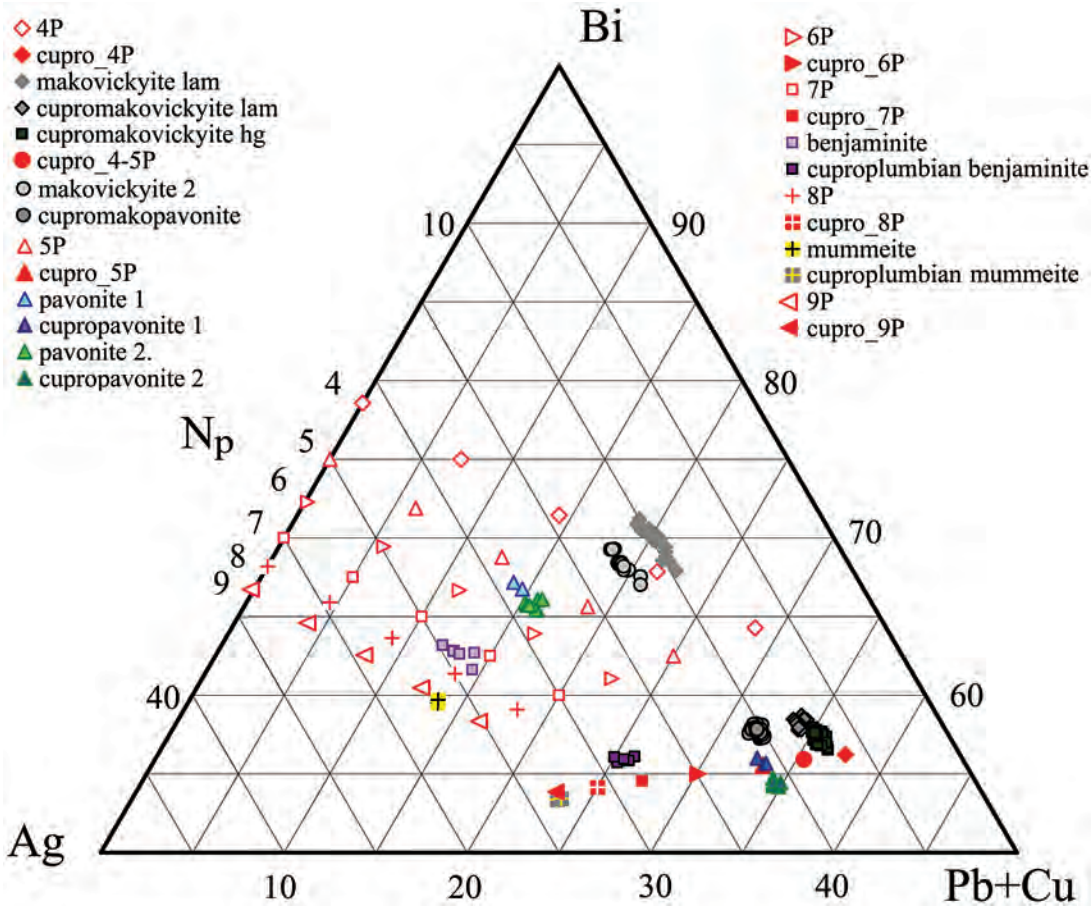

FIG. 10. Compositional scheme for pavonite homologues (void symbols) and cupropavonite homologues (solid symbols) in the Ag – Bi – (Cu + Pb) diagram. Lines for pavonite homologues of the order N_p are indicated by points at 0, 25, 50, 75 and 100 at.% of imaginary (Ag+Bi)-for-2Pb substitution by Pb in the octahedral cation sites, for Cu-free cases. Points indicating N_p values for the homologues of cupropavonite are situated on the ideal composition line for this series. Electron-microprobe data for the exsolution pairs are plotted into the scheme: makovickyite – cupromakovickyite from Băiţa Bihor, makovickyite – cupromakopavonite from Felbertal, pavonite – cupropavonite from the Alaska mine, Colorado, [1: Karup-Møller & Makovicky (1979) and 2: this work], benjaminite – cuproplumbian benjaminite from Erzwies (Makovicky *et al*. 2010), and mummeite – cuproplumbian mummeite from the Alaska mine (this work). Abbreviations: N_p: pavonite homologue with order value N, cupro-N_p: cupropavonite homologue with order value N, *lam*: lamellae, *hg*: homogeneous.

sive thickness of layers of octahedra or from a hasty exsolution or recrystallization of the minerals studied, is unknown at present. Interestingly, both cupropavonite and cuproplumbian mummeite come from the same locality, but from different museum samples.

On the chemical level, the cupropavonite homologous series and the substitutions in the pavonite homologous series may be modeled using the facts obtained from crystal-structure determinations (Table 10). From the ideal topology, occupancy and valence balance, the general formula of the cupropavonite homologous series is $Cu_8Ag_{2N-6}Pb_4Bi_{2N+10}S_{4N+20}$ for Z = 1, where N is the average of the N_1 and N_2 values in cases like cupromakopavonite. This ideal composition line is plotted in Figure 10 as a row of symbols for N = 4 to 9 (full symbols), together with the ideal compositions of respective pavonite homologues, in which Pb occupies 0, 25, 50, 75 and 100 percent of cation sites in the layer of octahedra (void symbols). The latter scheme works ideally for Cu-free homologues. Pavonite homologues that form exsolution pairs with the cuproplumbian ones are shown in Figure 10, as well. In general, they

show substitution percentages of about 75% or below; they all contain Cu in addition to Pb. Besides limitations imposed by stoichiometry of the thicker slabs, a potential misfit between the thicker and thinner slabs will limit the amount of Pb that can enter the octahedral positions of the thicker slabs.

Slight deviations of the members of the cupropavonite series from the ideal compositions may have experimental reasons (all data, except for those for homogeneous cupromakovickyite, come from exsolution lamellae alternating with a pavonite homologue) or may express a certain admixture of Bi in the Pb position of the thinner layers. The consistent trend of analytical results, closely parallel to the ideal composition line, confirms the constancy of structural and chemical principles involved; these are valid for both the strictly ordered, partly disordered and structurally not yet investigated members.

Conclusions

The rare Cu–Ag–Pb–Bi sulfosalt cupromakopavonite, a new mineral species, is closely related to cupromakovickyite and cupropavonite. It is a member $N_{1,2}$ = 4,5 (or N = 4.5) of the newly defined cupropavonite homologous series $Cu_8Ag_{2N-6}Pb_4Bi_{2N+10}S_{4N+20}$ for Z = 1, where N is the homologue order. Members with the order N from 4 to 8 are known. Although the topology of these structures resembles that of pavonite homologues, the homologues of cupropavonite have specific configurations of Pb and Cu that are distinct from those in the pavonite homologues. In the Ag–Bi–(Pb + Cu) diagram, the cupropavonite series assumes a compositional trend that is distinct from the homologues of pavonite. So far, cupromakopavonite is the only known member of the series, with two different values of N in the same structure.

Acknowledgements

There has been a crucial intersection between my mineralogical preoccupations and meeting and getting to know Emil Makovicky. As one of his Ph.D. students, I benefitted greatly from his insight and advice on the matter of sulfosalts, on how to approach the analytical side, and on how to get the most from the results. Ever since, Emil has been the most reliable scientific support for me, thus leading my research to numerous positive outcomes.

We gratefully acknowledge the financial support of the Christian Doppler Foundation (Austria) and the Research Council for the Nature and Universe, Denmark (grant no. 272–08–0227). The manuscript benefitted from comments of Prof. Giovanni Ferraris and Dr. Luca Bindi and from the editorial care of Prof. Robert F. Martin.

References

Balić-Žunić, T. & Makovicky, E. (1996): Determination of the centroid or 'the best centre' of a coordination polyhedron. *Acta Crystallogr.* **B52**, 78-81.

Balić-Žunić, T. & Makovicky, E. (2007): The crystal structure of kudriavite, $(Cd,Pb)Bi_2S_4$. *Can. Mineral.* **45**, 437-443.

Balić-Žunić, T. & Vicković, I. (1996): IVTON – program for the calculation of geometrical aspects of crystal structures and some crystal chemical applications. *J. Appl. Crystallogr.* **29**, 305-306.

Bente, K. & Kupcík, V. (1984): Redetermination and refinement of the structure of tetrabismuth tetracopper enneasulfide, $Cu_4Bi_4S_9$. *Acta Crystallogr.* **C40**, 1985-1986.

Bruker AXS (1998a): *SMART, Version 5.0*, Bruker AXS, Inc., Madison, Wisconsin 53719, USA.

Bruker AXS (1998b): *SAINT, Version 5.0*, Bruker AXS, Inc., Madison,Wisconsin 53719, USA.

Bruker AXS (1997): *XPREP, Version 5.1*, Bruker AXS, Inc., Madison,Wisconsin 53719,USA.

Chaplygin, I.V., Mozgova, N.N., Magazina, L.O., Kuznetsova, O.Yu., Safonov, Yu.G., Bryzgalov, I.A., Makovicky, E. & Balić-Žunić, T. (2005): Kudriavite, $(Cd,Pb)Bi_2S_4$, a new mineral species from Kudriavy volcano, Iturup Island, Kurile arc, Russia. *Can. Mineral.* **43**, 695-701.

Choe, Wonyoung, Lee, S., O'Connell, P. & Covey, A. (1997): Synthesis and structure of new Cd–Bi–S homologous series: a study in intergrowth and the control of twinning patterns. *Chem. Mater.* **9**, 2025-2030.

Ferraris, G., Makovicky, E. & Merlino, S. (2004): *Crystallography of Modular Materials*. I.U.C. Monographs on Crystallography, Oxford University Press, Oxford, U.K.

Herbert, H.K. & Mumme, W.G. (1981): Unsubstituted benjaminite from the Aw mine, New South Wales, a discussion of metal substitutions and stability. *Neues Jahrb. Mineral., Monatsh.*, 69-80.

Ilinca, G. & Makovicky, E. (1999): X-ray powder diffraction properties of pavonite homologues. *Eur. J. Mineral.* **11**, 691-708.

Karup-Møller, S. & Makovicky, E. (1979): On pavonite, cupropavonite, benjaminite and "oversubstituted" gustavite. *Bull. Minéral.* **102**, 351-367.

Karup-Møller, S. & Makovicky, E. (1992): Mummeite – a new member of the pavonite homologous series from Alaska mine, Colorado. *Neues Jahrb. Mineral., Monatsh.*, 555-576.

KRAUS, W. & NOLZE G. (1999): POWDERCELL 2.3. Federal Institute for Materials Research and Testing, Berlin, Germany.

MAKOVICKY, E. (1981): The building principles and classification of bismuth–lead sulphosalts and related compounds. *Fortschr. Mineral.* **59**, 137-190.

MAKOVICKY, E. (1989): Modular classification of sulphosalts – current status. Definition and application of homologous series. *Neues Jahrb. Mineral., Abh.* **160**, 269-297.

MAKOVICKY, E. (1997): Modular crystal chemistry of sulphosalts and other complex sulphides. *In* Modular Aspects of Minerals (S. Merlino, ed.). *Eur. Mineral. Union, Notes in Mineralogy* **1**, 237-271.

MAKOVICKY, E. (2006): Crystal structures of sulfides and other chalcogenides. *In* Sulfide Mineralogy and Geochemistry (D.J. Vaughan, ed.). *Rev. Mineral. Geochem.* **61**, 7-125.

MAKOVICKY, E. & BALIĆ-ŽUNIĆ, T. (1998): New measure of distortion for coordination polyhedra. *Acta Crystallogr.* **B54**, 766-773.

MAKOVICKY, E. & MUMME, W.G. (1979): The crystal structure of benjaminite $Cu_{0.5}Pb_{0.4}Ag_{2.3}Bi_{6.8}S_{12}$. *Can. Mineral.* **17**, 607-618.

MAKOVICKY, E., MUMME, W.G. & WATTS, J.A. (1977): The crystal structure of synthetic pavonite, $AgBi_3S_5$, and the definition of the pavonite homologous series. *Can. Mineral.* **15**, 339-348.

MAKOVICKY, E., PAAR, H.W., PUTZ, H. & ZAGLER, G. (2010): Dantopaite, $Ag_5Bi_{13}S_{22}$, the ^{6}P natural member of the pavonite homologous series, from Erzwies, Austria. *Can. Mineral.* **48**, 467-481.

MAKOVICKY, E., SØTOFTE, I. & KARUP-MØLLER, S. (2002): The crystal structure of $Cu_4Bi_4Se_9$. *Z. Kristallogr.* **217**, 597-604.

MOH, G.H. (1975): Tin-containing mineral systems. II. Phase relations and mineral assemblages in the Cu–Fe–Zn–Sn–S system. *Chem. Erde* **34**, 1-61.

MUMME, W.G. (1990): A note on the occurrence, composition and crystal structures of pavonite homologous series members ^{4}P, ^{6}P, and ^{8}P. *Neues Jahrb. Mineral., Monatsh.*, 193-204.

MUMME, W.G. & WATTS, J.A. (1980): $HgBi_2S_4$: crystal structure and relationship with the pavonite homologous series. *Acta Crystallogr.* **B36**, 1300-1304.

NUFFIELD, E.W. (1980): Cupropavonite from Hall's Valley, Park County, Colorado. *Can. Mineral.* **18**, 181-184.

SHELDRICK, G.M. (1997a): SHELXS–97. A computer program for crystal structure determination. University of Göttingen, Göttingen, Germany.

SHELDRICK, G.M. (1997b): SHELXL-97. A computer program for crystal structure refinement. University of Göttingen, Göttingen, Germany.

TAKEUCHI, Y. & OZAWA, T. (1974): The structure of $Cu_4Bi_4S_9$. *Proc. Japan Acad.* **50**, 751-755.

TOMEOKA, K., OHMASA, M. & SADANAGA, R. (1980): Crystal chemical studies on some compounds in the copper–bismuth sulfide Cu_2S–Bi_2S_3 system. *Mineral. J.* **10**, 57-70.

TOPA, D. (2001): *Mineralogy, Crystal Structure and Crystal Chemistry of the Bismuthinite–Aikinite Series from Felbertal, Austria*. Ph.D. thesis, Institute of Mineralogy, University of Salzburg, Austria.

TOPA, D., MAKOVICKY, E. & BALIĆ-ŽUNIĆ, T. (2003b): Crystal structures and crystal chemistry of the members of the cuprobismutite homologous series of sulfosalts. *Can. Mineral.* **41**, 1481-1501.

TOPA, D., MAKOVICKY, E. & BALIĆ-ŽUNIĆ, T. (2008): What's the reason for the doubled unit-cell volumes of copper–lead-rich pavonite homologues? The crystal structures of cupromakovickyite and makovickyite. *Can. Mineral.* **46**, 515-523.

TOPA, D., MAKOVICKY, E., BALIĆ-ŽUNIĆ, T. & PAAR, W.H. (2003a): Kupčikite, $Cu_{3.4}Fe_{0.6}Bi_5S_{10}$, a new Cu–Bi sulfosalt from Felbertal, Austria, and its crystal structure. *Can. Mineral.* **41**, 1155-1166.

TOPA, D., MAKOVICKY, E. & PAAR, W.H. (2002): Compositional ranges and exsolution pairs for the members of the bismuthinite–aikinite series from Felbertal, Austria. *Can. Mineral.* **40**, 849-869.

TOPA, D. & PAAR, W.H. (2008): Cupromakovickyite, $Cu_8Pb_4Ag_2Bi_{18}S_{36}$, a new mineral of the pavonite homologous series. *Can. Mineral.* **46**, 503-514.

ŽÁK, L., FRÝDA, J., MUMME, W.G. & PAAR, W.H. (1994): Makovickyite, $Ag_{1.5}Bi_{5.5}S_9$ from Băiţa Bihorului, Romania. The ^{4}P natural member of the pavonite series. *Neues Jahrb. Mineral., Abh.* **168**, 147-169.

Received September 17, 2010, revised manuscript accepted March 10, 2012.

```
data_cupromakopavonite

_audit_creation_method            SHELXL-97
_chemical_name_systematic
;
 ?
;
_chemical_name_common             ?
_chemical_melting_point           ?
_chemical_formula_moiety          ?
_chemical_formula_sum
 'Ag3 Bi19 Cu8 Pb4 S38'
_chemical_formula_weight          6849.59

loop_
 _atom_type_symbol
 _atom_type_description
 _atom_type_scat_dispersion_real
 _atom_type_scat_dispersion_imag
 _atom_type_scat_source
 'S'  'S'   0.1246   0.1234
 'International Tables Vol C Tables 4.2.6.8 and 6.1.1.4'
 'Cu'  'Cu'   0.3201   1.2651
 'International Tables Vol C Tables 4.2.6.8 and 6.1.1.4'
 'Ag'  'Ag'  -0.8971   1.1015
 'International Tables Vol C Tables 4.2.6.8 and 6.1.1.4'
 'Pb'  'Pb'  -3.3944  10.1111
 'International Tables Vol C Tables 4.2.6.8 and 6.1.1.4'
 'Bi'  'Bi'  -4.1077  10.2566
 'International Tables Vol C Tables 4.2.6.8 and 6.1.1.4'

_symmetry_cell_setting            'Monoclinic'
_symmetry_space_group_name_H-M    'C2/m  '

loop_
 _symmetry_equiv_pos_as_xyz
 'x, y, z'
 '-x, y, -z'
 'x+1/2, y+1/2, z'
 '-x+1/2, y+1/2, -z'
 '-x, -y, -z'
 'x, -y, z'
 '-x+1/2, -y+1/2, -z'
 'x+1/2, -y+1/2, z'

_cell_length_a                    13.3801(19)
_cell_length_b                    4.0007(6)
_cell_length_c                    31.083(4)
_cell_angle_alpha                 90.00
_cell_angle_beta                  93.064(2)
_cell_angle_gamma                 90.00
_cell_volume                      1661.5(4)
_cell_formula_units_Z             1
_cell_measurement_temperature     297(2)
```

```
_cell_measurement_reflns_used     ?
_cell_measurement_theta_min       ?
_cell_measurement_theta_max       ?

_exptl_crystal_description        ?
_exptl_crystal_colour             ?
_exptl_crystal_size_max           ?
_exptl_crystal_size_mid           ?
_exptl_crystal_size_min           ?
_exptl_crystal_density_meas       ?
_exptl_crystal_density_diffrn     6.846
_exptl_crystal_density_method     'not measured'
_exptl_crystal_F_000              2886
_exptl_absorpt_coefficient_mu     64.746
_exptl_absorpt_correction_type    ?
_exptl_absorpt_correction_T_min   ?
_exptl_absorpt_correction_T_max   ?
_exptl_absorpt_process_details    ?

_exptl_special_details
;
 ?
;

_diffrn_ambient_temperature       297(2)
_diffrn_radiation_wavelength      0.71073
_diffrn_radiation_type            MoK\a
_diffrn_radiation_source          'fine-focus sealed tube'
_diffrn_radiation_monochromator   graphite
_diffrn_measurement_device_type   ?
_diffrn_measurement_method        ?
_diffrn_detector_area_resol_mean  ?
_diffrn_standards_number          ?
_diffrn_standards_interval_count  ?
_diffrn_standards_interval_time   ?
_diffrn_standards_decay_%         ?
_diffrn_reflns_number             7811
_diffrn_reflns_av_R_equivalents   0.0978
_diffrn_reflns_av_sigmaI/netI     0.0754
_diffrn_reflns_limit_h_min        -17
_diffrn_reflns_limit_h_max        17
_diffrn_reflns_limit_k_min        -5
_diffrn_reflns_limit_k_max        5
_diffrn_reflns_limit_l_min        -40
_diffrn_reflns_limit_l_max        41
_diffrn_reflns_theta_min          1.97
_diffrn_reflns_theta_max          28.29
_reflns_number_total              2215
_reflns_number_gt                 1834
_reflns_threshold_expression      >2sigma(I)

_computing_data_collection        ?
_computing_cell_refinement        ?
_computing_data_reduction         ?
_computing_structure_solution     'SHELXS-97 (Sheldrick, 1990)'
```

```
_computing_structure_refinement   'SHELXL-97 (Sheldrick, 1997)'
_computing_molecular_graphics     ?
_computing_publication_material   ?

_refine_special_details
;
 Refinement of F^2^ against ALL reflections.  The weighted R-factor wR and
 goodness of fit S are based on F^2^, conventional R-factors R are based
 on F, with F set to zero for negative F^2^. The threshold expression of
 F^2^ > 2sigma(F^2^) is used only for calculating R-factors(gt) etc. and is
 not relevant to the choice of reflections for refinement.  R-factors based
 on F^2^ are statistically about twice as large as those based on F, and R-
 factors based on ALL data will be even larger.
;

_refine_ls_structure_factor_coef  Fsqd
_refine_ls_matrix_type            full
_refine_ls_weighting_scheme       calc
_refine_ls_weighting_details
 'calc w=1/[\s^2^(Fo^2^)+(0.0335P)^2^+0.0000P] where P=(Fo^2^+2Fc^2^)/3'
_atom_sites_solution_primary      direct
_atom_sites_solution_secondary    difmap
_atom_sites_solution_hydrogens    geom
_refine_ls_hydrogen_treatment     mixed
_refine_ls_extinction_method      SHELXL
_refine_ls_extinction_coef        0.000000(17)
_refine_ls_extinction_expression
 'Fc^*^=kFc[1+0.001xFc^2^\l^3^/sin(2\q)]^-1/4^'
_refine_ls_number_reflns          2215
_refine_ls_number_parameters      115
_refine_ls_number_restraints      0
_refine_ls_R_factor_all           0.0600
_refine_ls_R_factor_gt            0.0453
_refine_ls_wR_factor_ref          0.0952
_refine_ls_wR_factor_gt           0.0899
_refine_ls_goodness_of_fit_ref    1.018
_refine_ls_restrained_S_all       1.018
_refine_ls_shift/su_max           1.644
_refine_ls_shift/su_mean          0.014

loop_
 _atom_site_label
 _atom_site_type_symbol
 _atom_site_fract_x
 _atom_site_fract_y
 _atom_site_fract_z
 _atom_site_U_iso_or_equiv
 _atom_site_adp_type
 _atom_site_occupancy
 _atom_site_symmetry_multiplicity
 _atom_site_calc_flag
 _atom_site_refinement_flags
 _atom_site_disorder_assembly
 _atom_site_disorder_group
Ag Ag 0.0000 0.0000 0.0000 0.0340(9) Uani 0.937(12) 4 d SP . .
```

```
Bi Bi 0.0000 0.0000 0.0000 0.0340(9) Uani 0.063(12) 4 d SP . .
Bi1 Bi 0.27808(5) 0.0000 0.05767(2) 0.01379(18) Uani 1 2 d S . .
Bi2 Bi 0.44173(5) 0.0000 0.88385(2) 0.01332(18) Uani 1 2 d S . .
Bi3 Bi 0.18026(5) 0.0000 0.78873(2) 0.0181(2) Uani 1 2 d S . .
Pb Pb 0.28681(6) 0.0000 0.33522(3) 0.0299(2) Uani 1 2 d S . .
Bi4 Bi 0.42586(6) 0.0000 0.58778(3) 0.0206(3) Uani 0.803(8) 2 d SP . .
Ag4 Ag 0.42586(6) 0.0000 0.58778(3) 0.0206(3) Uani 0.197(8) 2 d SP . .
Bi5 Bi 0.14238(6) 0.0000 0.53161(3) 0.0202(3) Uani 0.855(9) 2 d SP . .
Ag5 Ag 0.14238(6) 0.0000 0.53161(3) 0.0202(3) Uani 0.145(9) 2 d SP . .
Cu1 Cu 0.05663(18) 0.0000 0.22566(9) 0.0295(6) Uani 1 2 d S . .
Cu2 Cu 0.48852(19) 0.0000 0.71336(9) 0.0294(6) Uani 1 2 d S . .
S1 S 0.3537(3) 0.0000 0.97120(15) 0.0162(10) Uani 1 2 d S . .
S2 S 0.0742(4) 0.0000 0.92146(18) 0.0226(11) Uani 1 2 d S . .
S3 S 0.1977(3) 0.0000 0.13651(14) 0.0122(9) Uani 1 2 d S . .
S4 S 0.4906(3) 0.0000 0.19396(14) 0.0142(9) Uani 1 2 d S . .
S5 S 0.2194(3) 0.0000 0.24820(15) 0.0137(9) Uani 1 2 d S . .
S6 S 0.0745(3) 0.0000 0.71698(14) 0.0122(9) Uani 1 2 d S . .
S7 S 0.3553(3) 0.0000 0.66526(16) 0.0166(9) Uani 1 2 d S . .
S8 S 0.0611(3) 0.0000 0.60653(16) 0.0170(10) Uani 1 2 d S . .
S9 S 0.2245(4) 0.0000 0.44028(18) 0.0231(11) Uani 1 2 d S . .
S10 S 0.5000 0.0000 0.5000 0.0199(14) Uani 1 4 d S . .

loop_
 _atom_site_aniso_label
 _atom_site_aniso_U_11
 _atom_site_aniso_U_22
 _atom_site_aniso_U_33
 _atom_site_aniso_U_23
 _atom_site_aniso_U_13
 _atom_site_aniso_U_12
Ag 0.0299(15) 0.0406(15) 0.0310(16) 0.000 -0.0015(10) 0.000
Bi 0.0299(15) 0.0406(15) 0.0310(16) 0.000 -0.0015(10) 0.000
Bi1 0.0159(4) 0.0118(3) 0.0137(4) 0.000 0.0013(3) 0.000
Bi2 0.0158(4) 0.0117(3) 0.0126(4) 0.000 0.0022(3) 0.000
Bi3 0.0195(4) 0.0210(4) 0.0133(4) 0.000 -0.0031(3) 0.000
Pb 0.0349(5) 0.0179(4) 0.0376(5) 0.000 0.0080(4) 0.000
Bi4 0.0246(5) 0.0204(5) 0.0170(5) 0.000 0.0019(3) 0.000
Ag4 0.0246(5) 0.0204(5) 0.0170(5) 0.000 0.0019(3) 0.000
Bi5 0.0208(5) 0.0179(5) 0.0218(5) 0.000 -0.0003(3) 0.000
Ag5 0.0208(5) 0.0179(5) 0.0218(5) 0.000 -0.0003(3) 0.000
Cu1 0.0230(13) 0.0294(14) 0.0350(17) 0.000 -0.0085(12) 0.000
Cu2 0.0294(14) 0.0163(12) 0.0411(17) 0.000 -0.0094(12) 0.000
S1 0.017(2) 0.017(2) 0.015(2) 0.000 0.0036(19) 0.000
S2 0.019(2) 0.014(2) 0.034(3) 0.000 -0.004(2) 0.000
S3 0.015(2) 0.015(2) 0.007(2) 0.000 0.0002(17) 0.000
S4 0.019(2) 0.014(2) 0.010(2) 0.000 0.0043(18) 0.000
S5 0.012(2) 0.014(2) 0.015(2) 0.000 -0.0006(17) 0.000
S6 0.014(2) 0.0108(19) 0.012(2) 0.000 -0.0005(17) 0.000
S7 0.017(2) 0.013(2) 0.020(3) 0.000 0.0018(19) 0.000
S8 0.018(2) 0.016(2) 0.016(2) 0.000 -0.0004(19) 0.000
S9 0.019(2) 0.013(2) 0.036(3) 0.000 -0.004(2) 0.000
S10 0.022(3) 0.018(3) 0.020(4) 0.000 0.000(3) 0.000

_geom_special_details
;
```